# NAVAL POSTGRADUATE SCHOOL

## Monterey, California






# THESIS

CLUSTER MODEL OF
POLARIZATION UPON REFLECTION
FROM METALLIC SURFACES

by

Craig Wesley Baldwin

December, 1991

Thesis Advisor: Oscar Biblarz

Approved for public release; distribution is unlimited

UNCLASSIFIED

SECURITY CLASSIFICATION OF THIS PAGE

# REPORT DOCUMENTATION PAGE

| | |
|---|---|
| 1a REPORT SECURITY CLASSIFICATION<br>Unclassified | 1b RESTRICTIVE MARKINGS |
| 2a SECURITY CLASSIFICATION AUTHORITY | 3 DISTRIBUTION/AVAILABILITY OF REPORT<br>Approved for public release; distribution is unlimited. |
| 2b DECLASSIFICATION/DOWNGRADING SCHEDULE | |
| 4 PERFORMING ORGANIZATION REPORT NUMBER(S) | 5 MONITORING ORGANIZATION REPORT NUMBER(S) |
| 6a NAME OF PERFORMING ORGANIZATION<br>Naval Postgraduate School<br>6b OFFICE SYMBOL (*If applicable*)<br>39 | 7a NAME OF MONITORING ORGANIZATION<br>Naval Postgraduate School |
| 6c ADDRESS (*City, State, and ZIP Code*)<br>Monterey, CA 93943-5000 | 7b ADDRESS (*City, State, and ZIP Code*)<br>Monterey, CA 93943-5000 |
| 8a NAME OF FUNDING/SPONSORING ORGANIZATION<br>8b OFFICE SYMBOL (*If applicable*) | 9 PROCUREMENT INSTRUMENT IDENTIFICATION NUMBER |
| 8c ADDRESS (*City, State, and ZIP Code*) | 10 SOURCE OF FUNDING NUMBERS<br>Program Element No / Project No / Task No / Work Unit Accession Number |

11 TITLE (*Include Security Classification*)
CLUSTER MODEL OF POLARIZATION UPON REFLECTION FROM METALLIC SURFACES (UNCLASSIFIED)

12 PERSONAL AUTHOR(S) Craig W. Baldwin, LCDR, USN

| 13a TYPE OF REPORT | 13b TIME COVERED | 14 DATE OF REPORT (*year, month, day*) | 15 PAGE COUNT |
|---|---|---|---|
| Master's Thesis | From To | December, 1991 | 69 |

16 SUPPLEMENTARY NOTATION
The views expressed in this thesis are those of the author and do not reflect the official policy or position of the Department of Defense or the U.S. Government.

| 17 COSATI CODES | | | 18 SUBJECT TERMS (*continue on reverse if necessary and identify by block number*) |
|---|---|---|---|
| FIELD | GROUP | SUBGROUP | Metallic Clusters Metallic Reflectors Micro Particles Finite Systems Polarization |
| | | | |
| | | | |

19 ABSTRACT (*continue on reverse if necessary and identify by block number*)

POLARIZATION OF LIGHT IS AT BEST ONLY PARTIALLY EXPLAINED BY CURRENT MODELS. A NEW MODEL IS PROPOSED TO ACCOUNT FOR THIS PHENOMONEN INVOLVING "NATIVE CLUSTERS". THESE CLUSTERS ARE ASSUMED TO BE AN INTEGRAL PART OF SOME BULK SURFACES AND TO MANIFEST THEIR DIELECTRIC PROPERTIES IN THE VISIBLE REGION. AN INDEX OF REFRACTION MAY BE COMPUTED BASED ON A PSEUDO-BREWSTER ANGLE, THAT ANGLE OF INCIDENCE WHERE THE MINIMUM PERPENDICULAR REFLECTANCE OCCURS. NEXT THE MODEL IDENTIFIES THE CLUSTER-TO-BULK SURFACE AREA RATIO OF THE MATERIAL AND FORMULATES THE CONTRIBUTION OF REFLECTION FROM THESE AREAS BY UTILIZING THE FRESNEL EQUATIONS. REFLECTANCE FROM THE REMAINDER, THE BULK-SURFACE AREA, IS COMPUTED BY APPLYING CONVENTIONAL METALLIC REFLECTION TECHNIQUES. BY COMBINING THE TWO CONTRIBUTIONS OF REFLECTANCE FOR ANGLES OF INCIDENCE FROM 0 TO 90 DEGREES, REFLECTANCE CURVES ARE GENERATED FOR GOLD, SILVER, NICKEL AND ALUNIMUM. THESE CALCULATIONS ASSUME A WIDE-BAND RADIATING SOURCE OF LIGHT. ALTHOUGH THE MAGNITUDE OF REFLECTANCE FOR THE MODEL SHOWED SOME VARIANCE OVER THE RANGE OF ANGLES OF INCIDENCE (1 WITHIN 10%), THE CURVES ARE SILMILAR IN SHAPE. THE MINIMUM PERPENDICULAR REFLECTANCE AND GRAZING ANGLES OF INCIDENCE ARE CONSISTENT WITH EXPERIMENTAL FINDINGS. THE COMPUTED SURFACE RATIO FOR EACH METAL VARIES INDIRECTLY WITH THE METAL'S NORMAL REFLECTANCE VALUE, AS EXPECTED FROM THE MODEL. SPECTRAL INFORMATION ON THE COMPLEX INDEX OF REFRACTION IS INCLUDED TO INFER PROBABLE CLUSTER SIZE.

| 20 DISTRIBUTION/AVAILABILITY OF ABSTRACT | 21 ABSTRACT SECURITY CLASSIFICATION | |
|---|---|---|
| ☒ UNCLASSIFIED/UNLIMITED ☐ SAME AS REPORT ☐ DTIC USERS | Unclassified | |
| 22a NAME OF RESPONSIBLE INDIVIDUAL<br>Oscar Biblarz | 22b TELEPHONE (*Include Area code*)<br>408-646-3906 | 22c OFFICE SYMBOL<br>AA/Bi |

**DD FORM 1473, 84 MAR** 83 APR edition may be used until exhausted
All other editions are obsolete

SECURITY CLASSIFICATION OF THIS PAGE
UNCLASSIFIED

Approved for public release; distribution is unlimited.

Cluster Model of
Polarization Upon Reflection
From Metallic Surfaces

by

Craig Wesley Baldwin
Lieutenant Commander, United States Navy
B.S., Purdue University 1979

Submitted in partial fulfillment
of the requirements for the degree of

MASTER OF SCIENCE IN ASTRONAUTICAL ENGINEERING

from the

NAVAL POSTGRADUATE SCHOOL
December, 1991

Author: Craig W. Baldwin
Craig W. Baldwin

Approved by: Oscar Biblarz
Oscar Biblarz, Thesis Advisor

Eugene Crittenden
Eugene Crittenden, Second Reader

Daniel J Collins
Daniel Collins, Chairman
Department of Aeronautics and Astronautics

## ABSTRACT

Polarization of light due to metallic reflection is at best only partially explained by current models. A new model is proposed to account for this phenomenon involving "native clusters". These clusters are assumed to be an integral part of metallic bulk surfaces and to manifest their dielectric properties in the visible region. An index of refraction may be computed based on a pseudo-Brewster angle, that angle of incidence where the minimum perpendicular reflectance occurs. Next the model identifies the cluster-to-bulk surface area ratio of the material and formulates the contribution of reflection from these areas by utilizing the Fresnel equations. Reflectance from the remainder, the bulk-surface area, is computed by applying conventional metallic reflection techniques. By combining the two contributions of reflectance for angles of incidence from 0 to 90 degrees, reflectance curves are generated for gold, silver, nickel and aluminum. These calculations assume a wide-band radiating source of light. Although the magnitude of reflectance for the model showed some variance over the range of angles of incidence (within 10%), the curves are similar in shape. The minimum perpendicular reflectance and grazing angles of incidence are consistent with experimental findings. The computed surface ratio for each metal varies indirectly with the metals' normal reflectance value, as expected from the model. Spectral information on the complex index of refraction is included to infer probable cluster size.


## TABLE OF CONTENTS

## ACKNOWLEDGMENTS

I would like to thank Professor Biblarz for the encouragement and patience allotted to me during my working with him on this thesis.

Further, I must thank Dennis and Dianne Norby, for opening their house to me for the last quarter while asking nothing in return, which permitted me the opportunity to spend the necessary time on my studies and thesis.

Finally, I wish to express my most heartfelt thanks to my wife JoAnn and my three loving children Allison, Adam and Ryan, for their love, understanding and encouragement while we were apart as I finished this theses. No man could be more proud than I am of you.

# I. DESCRIPTION OF MECHANISMS FOR METALLIC REFLECTION

## A. INTRODUCTION

Optical polarization was discovered by E. L. Malus in 1808. However, it was not until the nineteenth century and the formulation of electromagnetic theory developed by Maxwell that this phenomenon could be described analytically, at least partially. Moreover, the theory addresses the results more than the mechanism. J. Bennett and E. Bennett from the Naval Weapons Center are quoted in Ref. 1 as saying in reference to the electromagnetic theory,

> "This theory is phenomonological in that instead of trying to explain why materials have certain fundamental characteristics, it concentrates on the resulting properties which any material with those characteristics will display. Electromagnetic theory has little or nothing to say about why a material should have these particular optical properties ..."

This is a strong statement concerning the present lack of understanding involved in the polarization process during metallic reflection. Bennett and Bennett continue to state that at the present time solid state physics can only partially explain the mechanism which causes polarization for some surfaces. In this chapter, currently accepted mechanisms are mentioned and the concept of "native clusters" will be introduced.

## B. PRESENT SCOPE OF RESEARCH

Clusters are a collection of atoms which have properties between bulk and molecular entities. Clusters are also known as microparticles, or finite systems. They

are primarily studied in the free state [Ref. 2]. "Native clusters" [Ref. 3], refer to the covalent aggregation of a fixed number of atoms at the surface energy level of the metal. This clustering is presumed to exist at all times, although the cluster site position on the surface, varies with time.

Having performed a thorough literature search, and having been sponsored by the Naval Postgraduate school to attend an international symposium on the physics and chemistry of finite systems [Ref 4], the author has found that presently there is intense interest within the scientific community concerning clusters. However, despite the wide-ranging topic material presented at the conference [Ref. 4], there is a noticeable lack of research involving bound "native clusters" and their impact on surface science. It appears that the main thrust at present, is on defining, building and manipulating the free clusters, which are created through vaporization of bulk material by high energy lasers. Since, as stated in Refs. 2 & 4, free clusters are derived from the bulk material and by themselves display properties other than the bulk from which they were produced and that many clusters assembled together begin to take on the properties of the bulk, it seems logical that research involving "native clusters" would add to the understanding of how clusters, a distinct phase of matter [Ref 2], interact within metallic surfaces and modify their emission behavior.

## C. MECHANISMS OF POLARIZATION

Currently there are two accepted models which partially describe the behavior of reflected waves from metallic surfaces: The free electron theory which is best suited for

the infrared spectrum and below and, conversely the quantum model works well in the ultraviolet region of the energy spectrum and beyond.

### 1. Free Electron Theory

The free electron theory is based on a model where actually, two types of electrons reside on the surface. Bound electrons or electrons which are covalently bonded to the atoms which make up the crystalline surface of the metal and free electrons which are associated with good conductors and are free to move about in a random pattern thereby producing no net current [Ref. 5]. Introducing the complex index of refraction, the interaction of the free electrons with an electromagnetic wave can be accounted for by the imaginary part, which in turn depends on the properties of the metal. More specifically, on the conductivity as it relates to the number of free electrons in the metal [Ref. 5]. However, as one will note in Chapter III, the model is limited to the portion of the spectrum in the infrared (IR). However, two important facts are validated by this model.

- Electromagnetic waves in the near infrared and longer wavelengths are exclusively absorbed at the surface by interaction with the free electrons. (see Chapter III)
- Magnitudes of parallel and perpendicular polarized reflectance can be obtained from the Fresnel equations over the same portion of the energy spectrum given above.

### 2. Quantum Mechanics

For reasons explained in Chapter III the quantum model is best suited for explaining the mechanism in the ultraviolet (UV) and higher energy portion of the spectrum. High energy waves possess enough energy to influence conduction bands, it

is theorized, above the Fermi level but below the work function level. If this is the case then it may be possible to associate these bands with dipoles which are the necessary ingredient for polarization to occur. However, this linkage is not well developed at this time due to the complexity of the interaction between high frequency waves and the band electrons [Ref. 5].

### 3. Polarization Due To "Native Clusters"

"Native clusters" are postulated to exist as discrete sites on the surface, to be transparent and non-absorbing in the visible portion of the spectrum [Ref. 6]. The theory that "native clusters" do exist on metallic surfaces is proposed in Ref. 3. In this work, Bibiarz complements the free electron model used in describing thermionic emission from metals. It is postulated [Ref. 3], that clusters are intrinsic regions which exist on the surface of bulk metal and which alter all emission properties of the bulk (i.e., electron, atom and photonic). A thermionic model is developed which includes "native clusters" as a percentage of the total surface area of the metal. Combining the bulk contribution to the contribution from the clusters, the total thermionic emission is determined over a range of temperatures. As shown in Ref. 3, this model better predicts thermionic emission than the pure free electron model in the case of refractory metals.

The conjectured shape of clusters is interesting from the standpoint of their integration into the bulk surface. Clusters are mostly surface area. In fact Ref. 2 states that tightly packed clusters of 20 atoms may have only one atom in their interior. This would lead one to think of clusters as having much more surface than depth when composing a portion of the bulk metal. Further hampering the defining of the cluster

shape is the inability to observe cluster atomic structure directly with current electron microscopy methods if the cluster is less than about two nanometers in size [Ref. 4]. However, some cluster shapes are being inferred from mass spectral data and magic numbers associated with the material [Ref. 4].

If the cluster size is around one micrometer across [Ref. 3], then one can discount from being applicable to this model those portions of the spectrum which are made up of wavelengths either too big to affect the cluster or are so small that their interaction with the electrons in the cluster is negligible. For these portions of the spectrum, either the free electron model for long wavelengths or the quantum model for short wavelengths may be a more satisfactory explanation of the mechanism.

Free metallic clusters can be created through vaporization of the bulk metal by high energy lasers. Clusters created in this manner, when studied, do not have the same optical properties as the bulk [Ref. 2]. Therefore, it is reasonable to assume that clusters residing as a portion of the total metallic surface would not share the host optical properties and, in fact, could have the properties stated at the beginning of this chapter. Hence, it follows that if the clusters do exhibit dielectric behavior, their presence can be accounted for in the theory of electromagnetic radiation and by the Fresnel equations. By adding this portion to the contribution from the bulk (free electrons), total metallic reflectance may thus be determined. As such, a mechanism whereby waves of the near IR and visible portion of the spectrum are polarized, is established.

## II. BACKGROUND ON ELECTROMAGNETIC WAVE BEHAVIOR

When an electromagnetic wave encounters a boundary between two different optical media, such as an air-dielectric system, it is well known that the wave is resolved into two component parts, one being the reflected wave the other being the transmitted wave [Ref. 7]. In this work we consider "white" light and unpolarized electromagnetic waves, and as such, several properties of the wave as it encounters a dielectric boundary can be explained by electromagnetic theory based on Maxwell's equations [Ref. 5].

### A. INDEX OF REFRACTION

The speed of light in vacuum is defined and given by Equation 2.1 below.

$$c = \frac{1}{\sqrt{\mu_0 \varepsilon_0}} \qquad (2.1)$$

Where $\mu_0$ is the permeability of free space and $\varepsilon_0$ is the permitivity of free space.

For optical materials, the index of refraction is defined to be the ratio between the speed of light (c) in a vacuum and the speed of light in the medium (v) [Ref. 7] and is given below in Equation 2.2.

$$n = \frac{c}{v} \qquad (2.2)$$

However, for the derivations that follow it will be more correct to make a substitution for v in Equation 2.2 as follows: It is understood [Ref. 5] that for good dielectrics the magnetic permeability ($\mu$) of the dielectric is equal to the magnetic permeability of free

space. Therefore it follows from electromagnetic theory that the velocity of the wave (light) in the dielectric as given by Equation 2.3 [Ref. 7].

$$v = \frac{1}{\sqrt{\mu_0 \varepsilon'}} \tag{2.3}$$

Finally, by substitution of Equations 2.1 and 2.3 into Equation 2.2 the index of refraction for dielectrics is given by Equation 2.4.

$$n = \frac{\sqrt{\mu_0 \varepsilon'}}{\sqrt{\mu_0 \varepsilon_0}} = \sqrt{\frac{\varepsilon'}{\varepsilon_0}} \equiv \sqrt{\varepsilon} \tag{2.4}$$

For the remainder of this paper the permitivity term ($\varepsilon$) will refer to a relative permitivity defined as the ratio of permitivity of the dielectric over permitivity of free space.It should be noted that the index of refraction for dielectrics is a real number unlike the index of refraction for conductors which is given in complex form. The reason for this difference will become clear later.

The index of refraction is useful in defining a relationship between the angle of incidence ($\phi$) of the incident wave and the refraction angle ($\phi'$) of the refracted wave (Figure 2.1 ) known as Snell's law [Ref. 7].

$$\frac{\sin\phi}{\sin\phi'} = \frac{n'}{n} \tag{2.5}$$

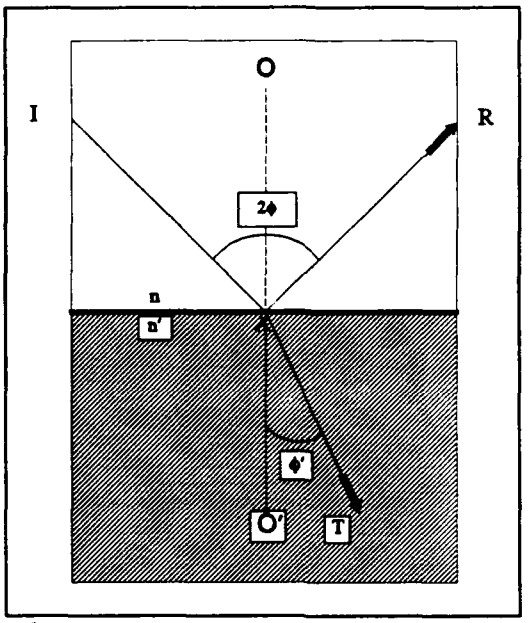


**Figure 2.1** Diagram Of Reflection And Refraction Between Two Optical Media n and n'

## B. FRESNEL EQUATIONS FOR DIELECTRICS

The description of the Fresnel equations for the transmitted and reflected light waves is straightforward and summarized below. A detailed derivation can be found in any book on electromagnetic wave propagation, such as Ref. 5.

Once a light wave encounters a dielectric boundary, the wave is split into two new waves. From Figure 2.1, one will note there is a reflected wave and a transmitted wave each with a parallel and perpendicular polarization component associated with it. If we let the amplitudes of the incident, reflected, and transmitted waves be denoted by I, R, T, respectively, as shown in Figure 2.1, then apply the boundary condition that the

tangential components be continuous across the boundary [Ref. 8], the results are given by Equation 2.6 [Ref 5].

Since the assumption was made in Ref. 8 that the clusters behave as a dielectric, $n' = \sqrt{\varepsilon}$. Making this substitution into the above equation and solving for $R_\perp$, $R_\parallel$, $T_\perp$, $T_\parallel$ the well known Fresnel equations for reflectance are obtained and given below by Equation 2.7.

$$\begin{aligned} \cos\phi' \, T_\parallel &= \cos\phi \, (A_\parallel - R_\parallel) \\ \sqrt{\varepsilon_2} \, T_\parallel &= \sqrt{\varepsilon_1} \, (A_\parallel + R_\parallel) \\ T_\perp &= A_\perp + R_\perp \\ \sqrt{\varepsilon_2} \cos\phi' \, T_\parallel &= \sqrt{\varepsilon_1} \, (A_\parallel + R_\parallel) \end{aligned} \qquad (2.6)$$

$$\begin{aligned} RSDP &= \left| \frac{R_\parallel}{A_\parallel} \right|^2 = \left[ \frac{\tan(\phi_i - \phi')}{\tan(\phi_i + \phi')} \right]^2 \\ RSDS &= \left| \frac{R_\perp}{A_\perp} \right|^2 = \left[ \frac{\sin(\phi_i - \phi')}{\sin(\phi_i + \phi')} \right]^2 \end{aligned} \qquad (2.7)$$

Note that RSDP and RSDS are reflectance coefficients and are the result of squaring the magnitudes of the intensities of the reflected and incident waves, as in evaluation of the pointing vector, then dividing by the square of the component amplitude of the incident wave which normalizes the equations.

## C. BREWSTER'S LAW FOR DIELECTRICS

Brewster's law simply states that there exists a specific angle of incidence which is material dependent, such that the reflected light from the dielectric is plane polarized

(i.e., RSDP = 0). From the top formula in Equations 2.7 one will note that this can only occur when the angle between the reflected and transmitted waves is 90° ($\phi_i + \phi' = 90°$) and hence the tangent goes to infinity. The definition of the Brewster angle, leads to Equation 2.8. This angle will be relevant to the development of the "native cluster" model, in Chapter IV.

$$\tan\theta = \frac{n'}{n} \qquad (2.8)$$

## D. REFLECTION AND REFRACTION PROPERTIES OF A CONDUCTOR

When an electromagnetic wave impinges on a metallic boundary (i.e., a good conductor) a surface current is immediately established . Unlike dielectrics, whose surface structure is composed of bound atoms and electrons, a conductor's surface is usually composed of small non orientated crystals containing free electrons. These free electrons will move so as to cause a surface current when in the presence of an external electric field.

### 1. Complex Index Of Refraction

According to [Ref. 5], by replacing the real index of refraction (n) as given in Equation 2.4, to a complex index of refraction (N) defined by Equation 2.9 an elementary model can be developed whereby the optical constants $\varepsilon$, $\sigma$, $\mu$, are utilized as in Equation 2.10, it defines the real and imaginary parts of the complex index of refraction. Note that $\sigma$ is the conductivity of the metal.

$$N = n - ik \tag{2.9}$$

$$n^2 = \frac{1}{2}\left[\sqrt{\mu^2 \varepsilon^2 + \frac{4\mu^2\sigma^2}{\nu^2}} + \mu\varepsilon\right]$$
$$n^2k^2 = \frac{1}{2}\left[\sqrt{\mu^2 \varepsilon^2 + \frac{4\mu^2\sigma^2}{\nu^2}} - \mu\varepsilon\right] \tag{2.10}$$

Work published in 1903 by E. Haygen and H. Rubens [Ref. 5] indicates that the results of Equations 2.10 are accurate for wavelengths of $10^{-3}$ cm (infrared waves) or longer. This however, will lead to some error between the calculated and experimental results of these optical properties in the visible to ultraviolet portion of the spectrum. Therefore, this model needs to be restricted to near infrared wavelengths. Notwithstanding the aforementioned, the complex index of refraction arises when dielectric electromagnetic theory is expanded to encompass conductors. Figure 2.2 from Ref. 1, shows the trends in the reflectance curves for increasing n and k. It is particularly helpful in showing that wave propagation into the conductor is small, and hence can be neglected. By defining the "skin-depth" (d) as the distance an electromagnetic wave will travel into a conductor before dissipation of it's energy to a value of 1/e, and linking this to the inverse of the extinction coefficient [Ref. 5], one can show that the distance of wave propagation into the medium is given by Equation 2.11.

$$d = \frac{c}{\sqrt{8\pi\mu\sigma\omega}} \tag{2.11}$$

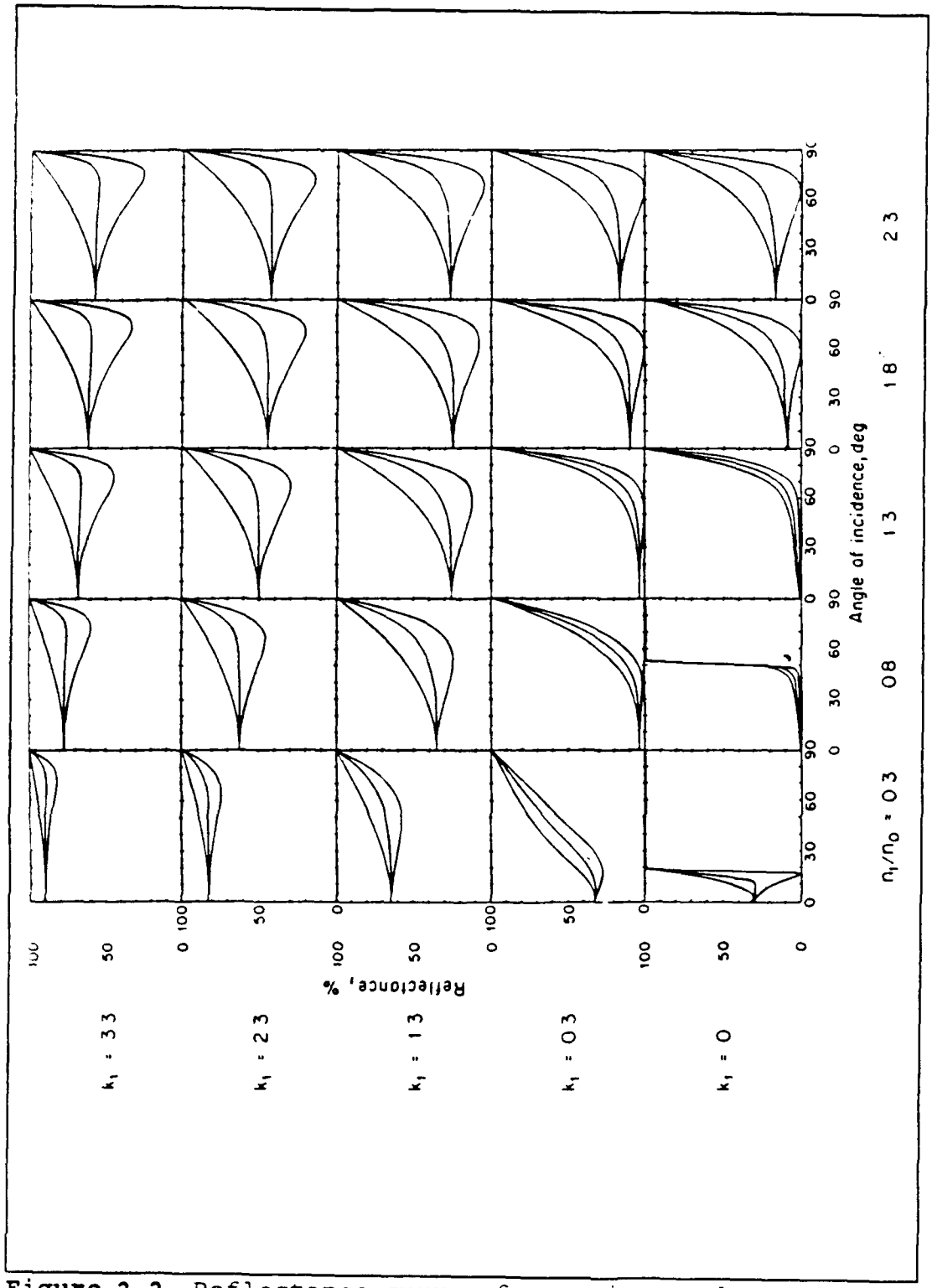


**Figure 2.2** Reflectance curves for various values of n and k derived from the free eiectron model.

From Equation 2.11, one will note that high conductivity (on the order of $10^{17}$ sec Gaussian units) and high frequencies, as in visible waves, will result in a very small skin depth. As proof an example of how little the wave will be transmitted into the conductor, Ref. 5 gives a skin depth of $d = 10^{-7}$ cm for infrared wave into copper a typical metallic conductor. This fact plays an important role in the development of the bulk reflection model as outlined in Chapter IV, since we can consider the metals to be opaque in the visible portion of the spectrum.

# III. FREE ELECTRON AND QUANTUM MODELS

## A. THE FREE ELECTRON MODEL OF METALLIC REFLECTION

In Chapter II, wave reflectance from a conductor was addressed using the classical electromagnetic theory based on Maxwell's equations, together with the introduction of the complex index of refraction. In this section the free electron model (proposed by P. Drude) will be shown and comments on its short comings in dealing with the higher frequency wave reflectance will be made.

The basis of the theory for the free electron model is that in a good conductor two types of electrons must reside at the surface. The first type are called bound electrons, or those which are held in a quasi-rigid state by the parent atom, similar to the dielectric. The second type, called free electrons, is a well established model for conductors, in that the surface is full of these electrons which are not bound to any atom and can move fairly freely about. As discussed in the previous chapter, the complex index of refraction is frequency dependent. However, Ref. 5 states that the complex conductivity and emissivity are both frequency dependent, which is shown by Equations 3.4 and 3.6.

### 1. Derivation Of The Complex Conductivity Term

From statistical methods of the theory of kinetics of gases, the motion of the free electrons can be described by a model of a proportional damping force acting in the opposite direction of the free electron motion [Ref 5]. This motion which is cyclic in nature due to the electric field being cyclic, can be described by the standard second

order differential equation of motion for a damped spring mass system under the influence of the forcing function **E** as shown below.

$$m\ddot{\vec{r}} + m\beta\dot{\vec{r}} = e\vec{E} \qquad (3.1)$$

The solution of Equation 3.1 is given in complex form below (i = imaginary index).

$$\vec{r} = -\left[\frac{e}{m(\omega^2 + i\beta\omega)}\right]\vec{E} \qquad (3.2)$$

Where **r** is the position vector of the periodic motion of frequency ($\omega$) the electron in an electric field with a damping coefficient ($\beta$). The decay time ($\tau$) is inversely related to the damping coefficient ($\beta$) which is on the order of $10^{-14}$ sec [Ref. 5]. Differentiating Equation 3.2, to obtain the velocity of the electron, and substituting this into Equation 3.3 below

$$\vec{J} = N_e e\dot{\vec{r}} = \left[\frac{N_e e^2}{m(\beta - i\omega)}\right]\vec{E} \qquad (3.3)$$

and finally using the constitutive relation between current density (**j**) and the electric field (**E**) viz. $\mathbf{j} = \sigma\mathbf{E}$ and substituting for $\sigma$ from Equation 3.3 the result is [Ref. 5]

$$\sigma = \frac{N_e e^2}{m(\beta - i\omega)} \qquad (3.4)$$

Note that $N_e$ is the number of free electrons in the conducting band. Thus the dependency on frequency for conductivity is established which will be important in the analysis of the model later in the chapter.

## 2. Complex Emissivity

As stated in Chapter II for conductors, the index of refraction is complex and since

$$n = \sqrt{\frac{\mu\varepsilon'}{\mu_0\varepsilon_0}} = \sqrt{\varepsilon} \qquad (3.5)$$

It follows that if the index of refraction is complex then, by definition as shown in Equation 3.5, so must the emissivity be complex. For low frequencies Ref. 5 states that the real part of $\varepsilon$ is small compared to the imaginary part and hence Equation 2.9 becomes the expression for the complex $\varepsilon$.

$$\hat{\varepsilon} \equiv N^2 = 1 - \left[\frac{4\pi N_e e^2}{m\omega(\omega - i\beta)}\right] \qquad (3.6)$$

Hence the dependence on frequency is again established as it was for the conductivity.

## 3. Analysis Of The Free Electron Model

The free electron model as presented predicts well the optical constants of the conductor for long wavelengths (IR, near or far), but does not accurately predict the behavior of the constants and hence, the reflection of the wave, in the visible portion of the energy spectrum. Evidence of this is presented in Ref. 5. The problem stems from the fact that Equation 3.6 as stated above is derived based on low frequency electric fields, in order to eliminate the contribution of the bound electrons. However, the contribution from the bound electrons becomes more significant as the frequency

increases thereby leading to the breakdown in the model. It is stated in Ref. 5 that the free electron model can not be modified in order to extend it's usefulness into the higher frequency ranges due to the complexity of the interaction between the electric field and the metal in these ranges. It refers the reader to the theory of quantum mechanics for an explanation.

## B. QUANTUM THEORY

Band theory of solids is presented in various references (see, for example, Ref. 9). For metals, the theory seems most appropriate in the violet and smaller wavelengths. Interband electron transitions in the near infrared are best known in semiconductors. The quantum mechanical expression for the polarizability is of the same form as that obtained from the classical (Drude) model.

Weak interband transitions appear to decrease the reflectance of aluminum around 1.4 eV . In silver, the reflectance, well into the "vacuum" ultraviolet region, is characteristic of interband transitions spread over a wide spectral region. At 3.9 eV a sharp decrease in reflectance identifies the free-electron plasma frequency. Plasma oscillations are a non-quantum, collective oscillation of the free electrons. Discussion of the present state of this field is beyond the scope of this work.

# IV. MODEL DEVELOPMENT

## A. "NATIVE CLUSTER" DESCRIPTION

"Native clusters" are postulated to be clusters which form not as a result of the presence of "foreign" atoms deposited on the surface, but rather because of an equilibrium of surface atom configurations [Ref. 3]. The "native cluster" model (Figure 4.1) is able to account for a number of the "nonconductor" properties of reflected light from metallic surfaces since in a cluster, the electrons remain attached to the atoms which make up the cluster and hence do not contribute to the Fermi level. Biblarz postulates in Ref. 6 that a patchwork of "native clusters" that exist on virgin metallic surfaces (based on work published in Ref. 3) does alter polarization upon metallic reflection . The dispersement of such "native clusters" over the bulk surface may produce dispersed dipoles thereby providing the surface with "nonconductor" attributes as exhibited by polarization, by the reflection of visible light from the surfaces, as well as other attributes.

## B. FORMULATION OF EQUATIONS

Based on Ref. 3, there is assumed to exist an equilibrium surface area ratio of cluster to bulk material unique to any given metal. Therefore reflected light will have contributions from the bulk ($r_B$) and clusters ($r_S$). The total surface area ($S_T$) is defined as the sum of the cluster area ($S_S$) and the bulk area ($S_B$) as shown in Equation 4.1.

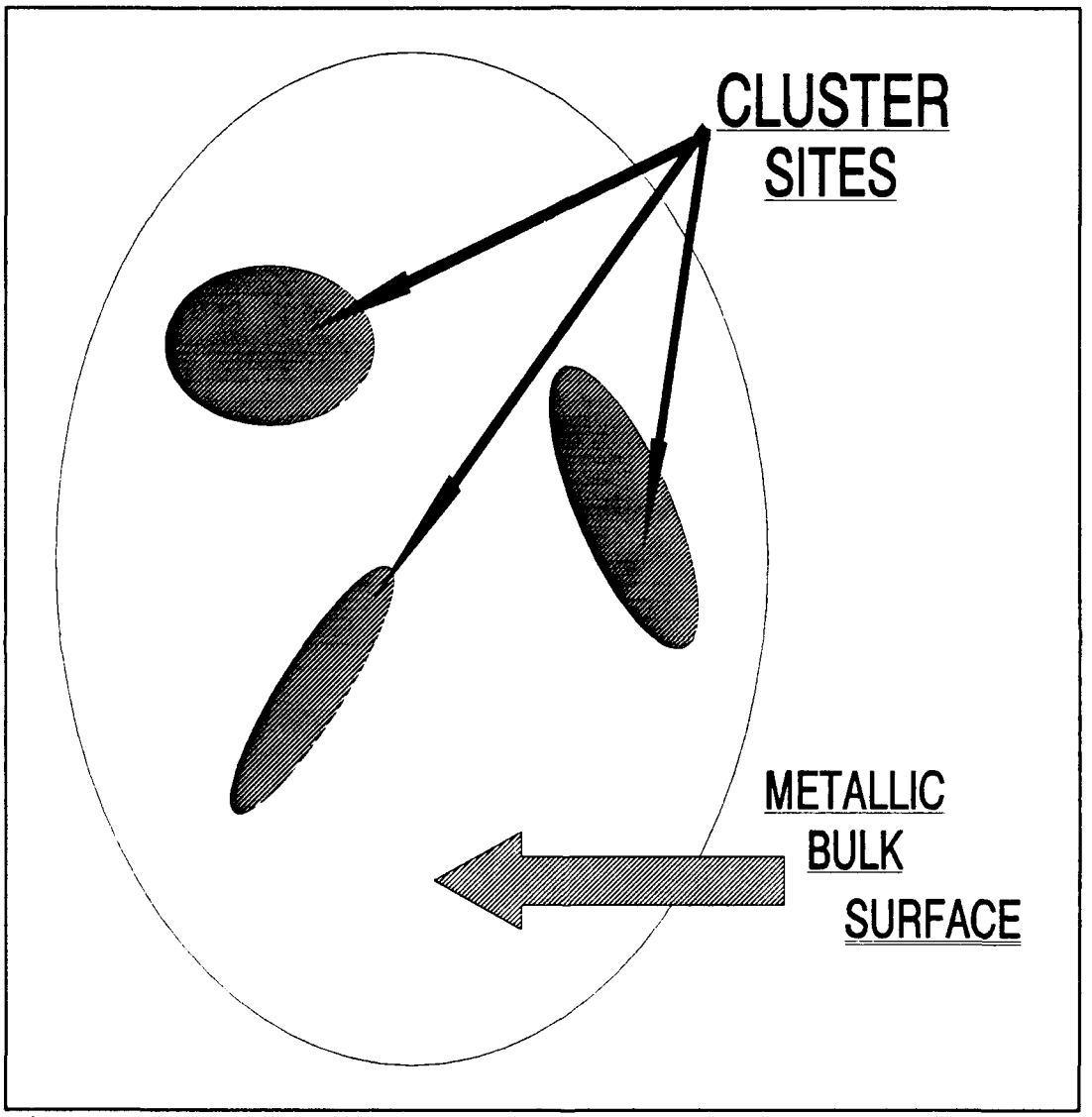


**Figure 4.1** Schematic Of Metallic Bulk Cluster Aggregate (Top View)

$$S_S + S_B = S_T \qquad (4.1)$$

Dividing Equation 4.1 by the total surface area (normalizing) and defining the fraction $S_S/S_T$ as x, the cluster to total surface ratio, one can substitute this value into Equation 4.1 and solve for the normalized bulk to total surface area ratio as in Equation 4.2.

$$(1 - x) = \frac{S_B}{S_T} \qquad (4.2)$$

Total reflectance ($r_T$) is then given in [Ref. 5] as

$$r_T = (1 - x) r_B + x r_S \qquad (4.3)$$

Since the bulk can be considered opaque in the near IR and visible portion of the spectrum [Ref. 6] (the skin depth being on the order of $10^{-7}$ cm), the contribution from the bulk is simply the reflectance of the bulk times it's normalized surface area. However, clusters behaving as dielectrics, are presumed to be transparent and will allow a portion of the waves to be transmitted through the cluster and then reflected by the metallic substrate while the remainder is reflected directly at the surface. As such, reflectance from the clusters maybe composed of direct reflectance ($r_{Sd}$) and indirect reflectance ($r_{Si}$) leading to

$$r_S = r_{Sd} + r_{Si} \qquad (4.4)$$

A gray body is defined to have characteristics of a black body where the absorptance is equal to the emittance. Assuming that the metallic surface behaves as a gray body (a good assumption for infrared to visible wavelengths) then the absorptance must equal the emissivity (Kirchhoff's law) [Ref. 1] as shown in Equation 4.5.

$$\alpha(\lambda, T) = \epsilon(\lambda, T) \tag{4.5}$$

Energy flux incident on surface can be reflected, transmitted, or absorbed. Applying Equation 4.5 to the flux balance equation [Ref. 1] the relationship between absorptance ($\alpha$ or $\epsilon$), reflectance (r) and transmittance ($\tau$) is shown to be

$$\epsilon(\lambda, \phi, T) + r(\lambda, \phi, T) + \tau(\lambda, \phi, T) = 1 \tag{4.6}$$

## C. BULK REFLECTANCE

Transmittance of the light wave into the bulk is shown to be negligible as stated in Ref. 5, hence Equation 4.6 may be written as

$$r_B = 1 - \epsilon(\lambda, T)\cos\phi \tag{4.7}$$

The angle of incidence ($\phi$) is defined as the angle between the incident ray and the normal to the surface (see Figure 2.1).

According to Ref. 6 the emittance is well represented in the IR region of the spectrum by Equation 4.8,

$$\epsilon(\lambda, T) \approx 36.5\sqrt{\rho\,(ohm\text{-}cm)/\lambda\ (\mu m)} \qquad (4.8)$$

where $\rho$ (a function of temperature) is the resistivity of the metal in ohm-cm and $\lambda$ is the wavelength of the incident wave in $\mu$m. The non-spectral form of the emmittance is determined by integrating over the entire spectrum and shown in Equation 4.9.

$$\epsilon\ (T) \cong 0.5753\sqrt{\rho\,(ohm\text{-}cm)\cdot T_S(K)} \qquad (4.9)$$

## D. CLUSTER REFLECTANCE

Native clusters possessing dielectric properties will cause incident waves to either be reflected directly ($r_{sd}$) or indirectly ($r_{si}$) after transmission through the cluster and reflection from the metallic substrate (see Figure 4.2). As shown by Equation 4.4.

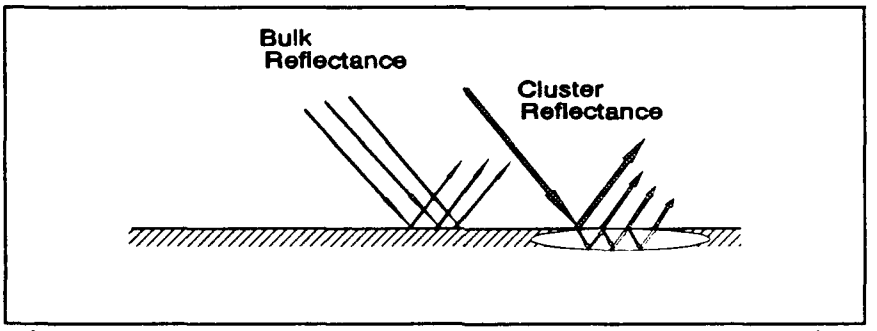


**Figure 4.2** Bulk and Cluster Reflection Patterns

### 1. Direct Cluster Reflectance

Direct cluster reflectance is calculated using the Fresnel equations for dielectrics [Ref. 7]. The reflected light has two components, parallel and perpendicular, representing the polarization effect upon reflection from a dielectric.

### 2. Indirect Cluster Reflectance

The indirect portion of the reflection is much more difficult to define as it requires knowledge of the shape and size of clusters. Some insight regarding the size of the "native cluster" is discussed in Chapter VI. No attempt was made to include this contribution but preliminary estimates indicate that the magnitude of the contribution to reflection will be on the order of 20% or less.

# V. COMPUTER MODEL DESIGN

## A. COMPUTER ALGORITHM DEVELOPMENT

Utilizing equations derived in Chapter IV, a computer algorithm named "REFLECTA" (see Appendix A) was developed to calculate the parallel (RTOTLS) and perpendicular (RTOTALP) reflectance from the metallic surface for angles of incidence from $0^{\circ}$ to $90^{\circ}$. Reflectance curves were generated from the data by invoking "Easy-Plot", a locally developed software package used with FORTRAN VII at the Naval Postgraduate School, and plotting RTOTLP or RTOTLS against the angle of incidence ($\phi$) for each metal.

## B. CURVE FITTING

White light reflectance curves for gold, and silver based on experimental results [Ref. 7], were considered to be the baseline from which the "native cluster" model could be compared to, then scrutinized for similarities and differences. Being able to produce reflectance curves from the model which matched the experimental curves, would be proof for the validation of the model.

Three parameters , bulk-cluster index of refraction (n'), cluster to bulk surface area ratio (x) and emittance ($\epsilon$) were utilized in obtaining the best curve fit for a particular metal.

## C. EQUATIONS USED IN COMPUTER ANALYSIS

Initially the parameters were fixed, based on results reported in Ref. 7 for gold and silver, which measured reflectance from a "white" tungsten light bulb, probably operating at 3000 K. Plots for these curves are shown in Chapter VI as Figures 6.1 and 6.2. However, curves were also generated for aluminum and nickel in order to expand the data base for future trend analysis (see Figures 6.3 and 6.4). Referring to the REFLECTA program, four terms were considered a critical part in plotting of the reflectance coefficient curves, and are defined below for continuity purposes as they will be repeatedly referred to in the remainder of the thesis.

- RTOTLP is the total surface parallel reflectance coefficient of the metallic surface.
- RTOTLS is the total surface perpendicular reflectance coefficient of the metallic surface.
- RSDP is the parallel reflectance coefficient contribution from direct cluster reflection (Equation 5.1).
- RSDS is the perpendicular reflectance coefficient contribution from direct cluster reflection (Equation 5.2).

RSDS and RSDP were calculated by Equations 5.1 and 5.2.

$$RSDS = \left[\frac{\sin(\phi - \phi')}{\sin(\phi + \phi')}\right]^2 \qquad (5.1)$$

$$RSDP = \left[\frac{\tan(\phi - \phi')}{\tan(\phi + \phi')}\right]^2 \qquad (5.2)$$

From Equations 5.3 and 5.4, RTOTLP and RTOTLS were calculated.

$$RTOTLS = (1 - x)RB + xRSDS \quad (5.3)$$

$$RTOTLP = (1 - x)RB + xRSDP \quad (5.4)$$

It was noted that the angle of incidence where RTOTLP was a minimum occurred about four degrees right of the experimental curve given in Ref. 7. By noting that this minimum is associated with the pseudo-Brewster angle for the metal, as defined by the minimum perpendicular reflectance as shown in Ref. 7, calculation of the index of refraction for the bulk-cluster aggregate (n′) is determined by the following equation.

$$n' = n_1 Tan\phi_{min} \quad (5.5)$$

where $\phi_{min}$ is the pseudo-Brewster angle and $n_1$ is the index of refraction of air or vacuum (equal to 1.0). However, by adjusting the incident angle to match the experimental pseudo-Brewster angle the entire reflectance curve was shifted up or down depending on the direction of shift in $\phi$ caused by the matching of the pseudo- Brewster angle. At this point it became clear that a sensitivity analysis for each parameter was required in order to formulate a systematic approach whereby, the three parameters could be varied in a convergent manner thus providing the best curve fit by the model.

## D. SENSITIVITY ANALYSIS OF PARAMETERS

As stated above in Section B of this chapter, due to the interdependence of the three parameters used in the generation of the curves and their complexity it is necessary

to perform an analysis on each parameter in order to determine what effect a small change in each has on the reflectance curves.

### 1. Procedure

Sensitivity testing was performed using gold, by varying one parameter in small increments while holding the other two constant. Total reflectance was recorded at two angles of incidence each chosen for their critical nature in the curve. The first was at $\phi = 2°$ where the incident light is virtually normal and hence the $\cos(\phi)$ is nearly one thereby eliminating the dependence of angle of incidence at that point. The second is located at a point where RTOTLP is at a minimum since, this will provide the best information on curve shifts due to small parameter changes at the Brewster angle. It is felt that the best curve fit would be obtained if these points could be made to match with experimental results.

### 2. Findings From Sensitivity Analysis

The results of the sensitivity testing are shown in Figure 5.1 and are summarized below.

- Small changes in the parameters produced linear increments of change in the curves.
- Increasing x decreased RTOTLP at $\phi = 2°$ and the minimum RTOTLP. There was no change in $\phi_{min}$, which was expected since this is governed by n' only.
- Varying $\epsilon$ had no effect on the shape of the curves. Thus this parameter can be determined by Equation 4.9 and fixed.
- Increasing n' increases RTOTLP at $\phi = 2°$; produces no change in $RTOTLP_{min}$; and increases $\phi_{min}$.

### 3. Partial Conclusions From Sensitivity Analysis

From the displayed linearity above and the equation of a line we can generate two simultaneous equations. Letting y be the value of RTOTLP at an angle of incidence equal to 2°, we can solve for the two unknowns, slope of the line (m) and the intercept (b) for a given n′, set initially by the pseudo-Brewster angle. Once this is accomplished, the value for x can be determined for that metal by setting y equal to the experimental value of RTOTLP at normal incidence and solving for x. The curves are then generated using these parameter values. The angle of incidence corresponding to $RTOTLP_{min}$ is compared with the experimental value and a small change is made in n′ in order to shift the curve towards the experimental. This new n′ is then used in determining a new value for x and the process repeats itself until $\phi_{min}$ experimental matches with that of the program. It's important to note at this time that the initial estimate of x should be chosen so as to comply with current wisdom regarding the area ratio of cluster to bulk.

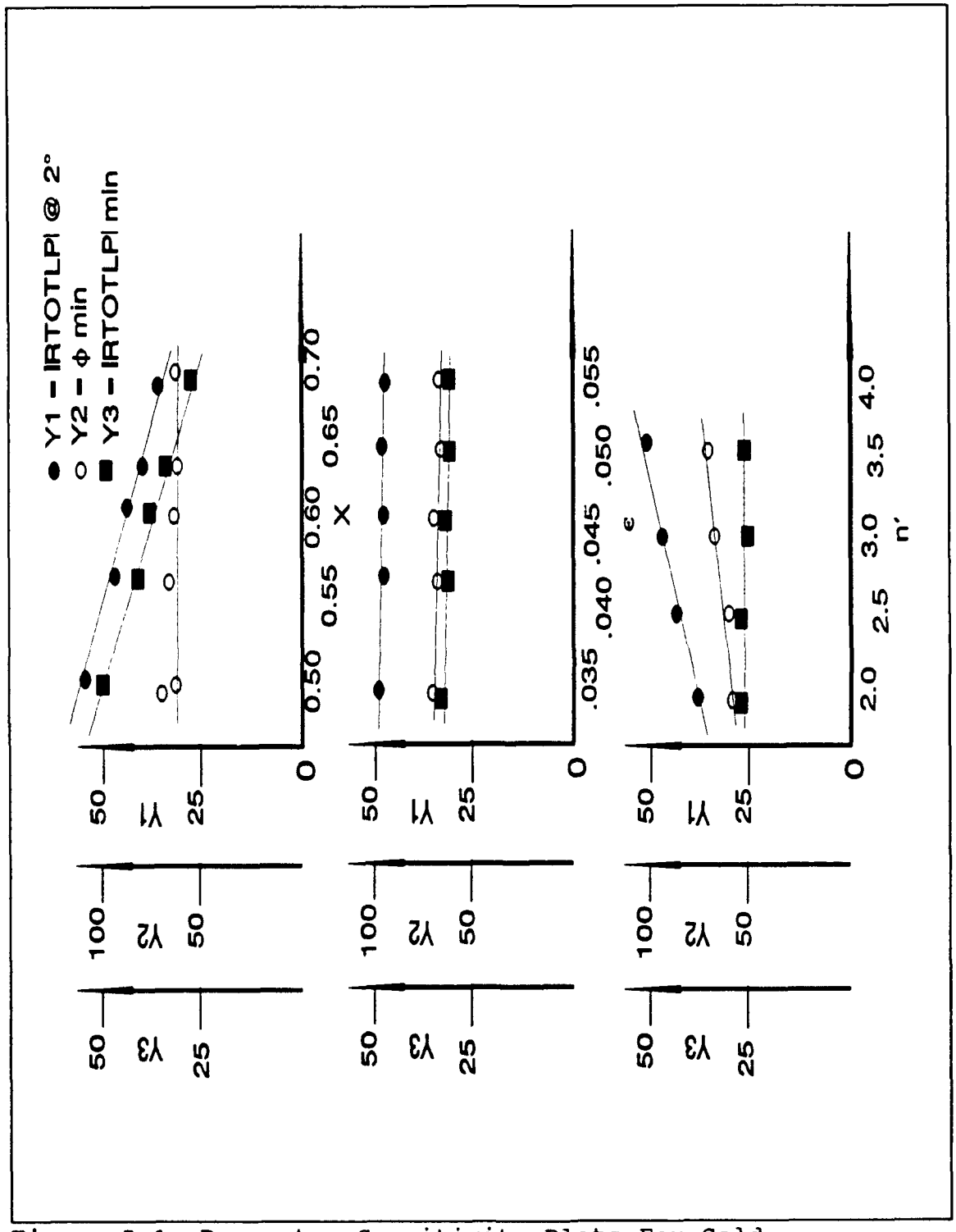


**Figure 5.1** Parameter Sensitivity Plots For Gold

# VI. RESULTS

## A. CURVE FIT EXPERIMENTAL VERSUS THE MODEL

Utilizing the aforementioned "native cluster" model and the computer algorithm developed in the previous chapter, total reflectance curves were generated for four metals, gold, aluminum, nickel, and silver (Figures 6.1 thru 6.4). These data as well the results produced by the model are for wide-band light (i.e., white light) where the source temperature was assumed to be 3000 K. Experimental values for gold and silver are shown as x's. The definition of these parameters is necessary in order to incorporate the experimental curves displayed in Ref. 7, for comparison purposes to those of the model.

Comparison of the reflectance curves produced by the model to the experimental curves given in Ref. 6 reveal the following similarities listed below.

- At normal incidence ($\phi = 0°$), both parallel and perpendicular reflectance have the same magnitudes. Further, this common magnitude is in agreement with the value measured by experimental means.
- Perpendicular reflectance increases as the angle of incidence increases throughout the range of values in a similar fashion to the experimental values.
- Parallel reflectance decreases to a minimum located at an angle of incidence associated with the pseudo Brewster angle of the metal as does the experimental value of parallel reflectance.
- Parallel reflectance increases for angles of incidence greater than the pseudo-Brewster angle to the grazing angle of incidence ($\phi = 90°$).

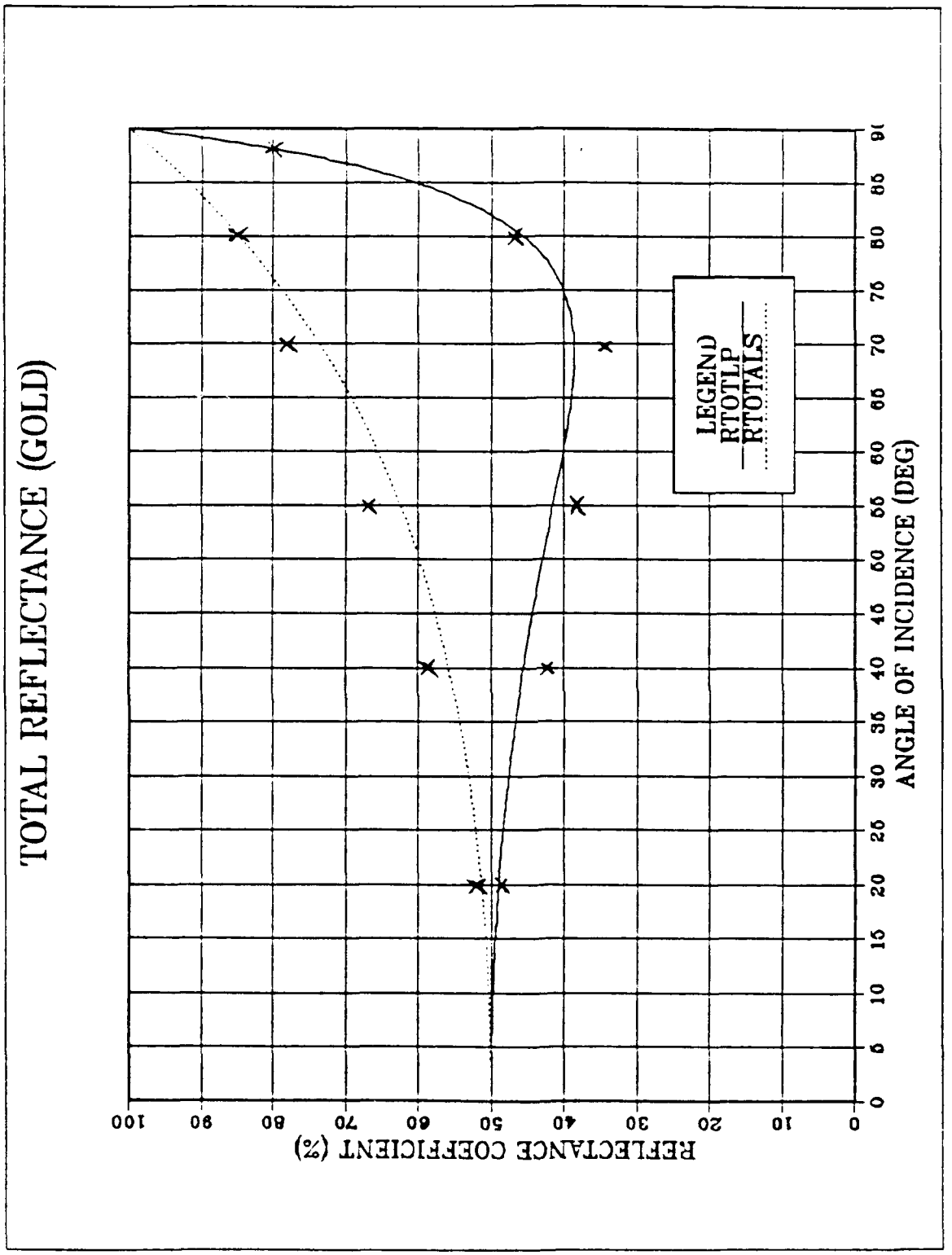


**Figure 6.1** Reflectance Curves Of Gold. x's correspond to measurements from Ref. 7.

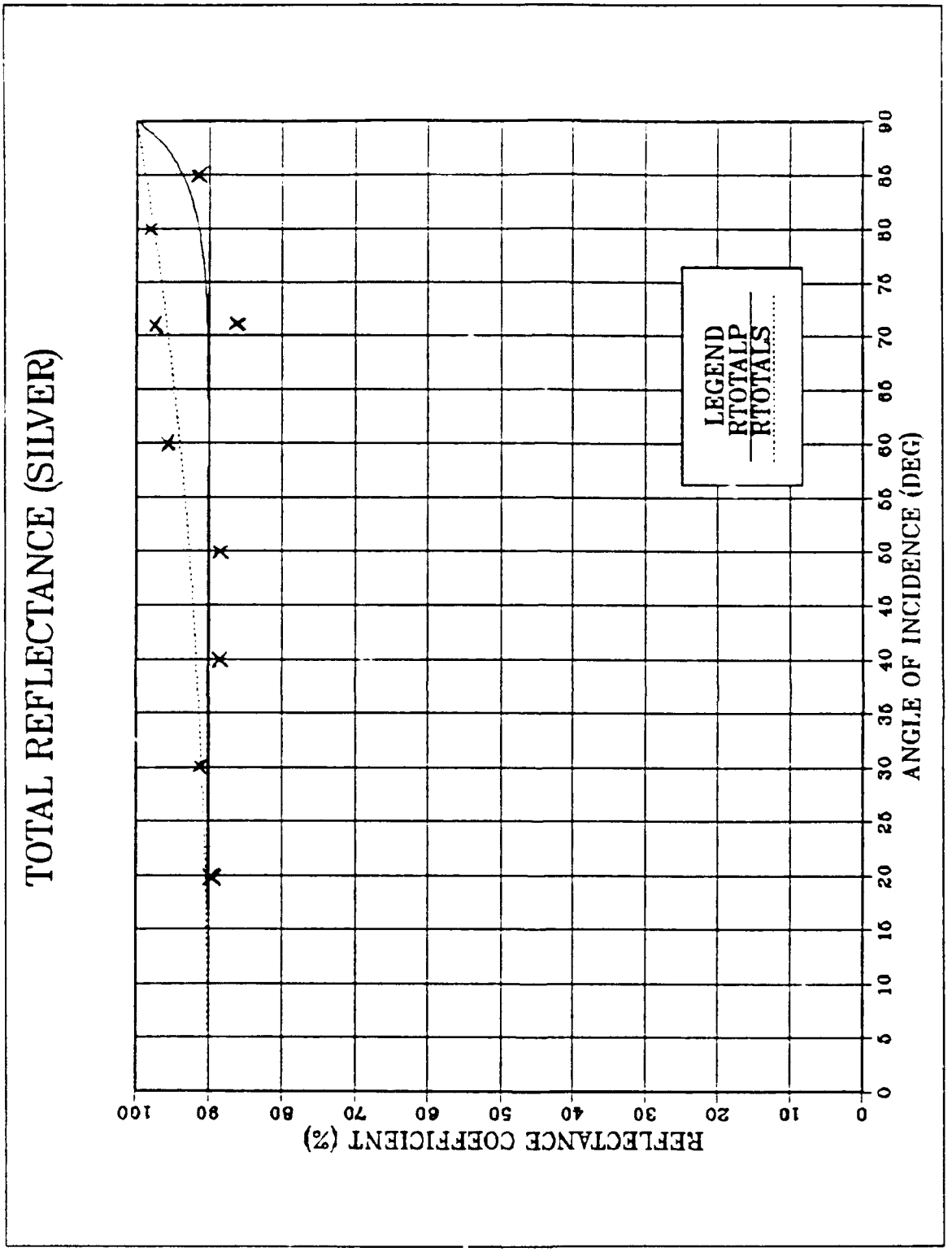


**Figure 6.2** Reflectance Curves Of Silver. x's correspond to measurements from Ref. 7.

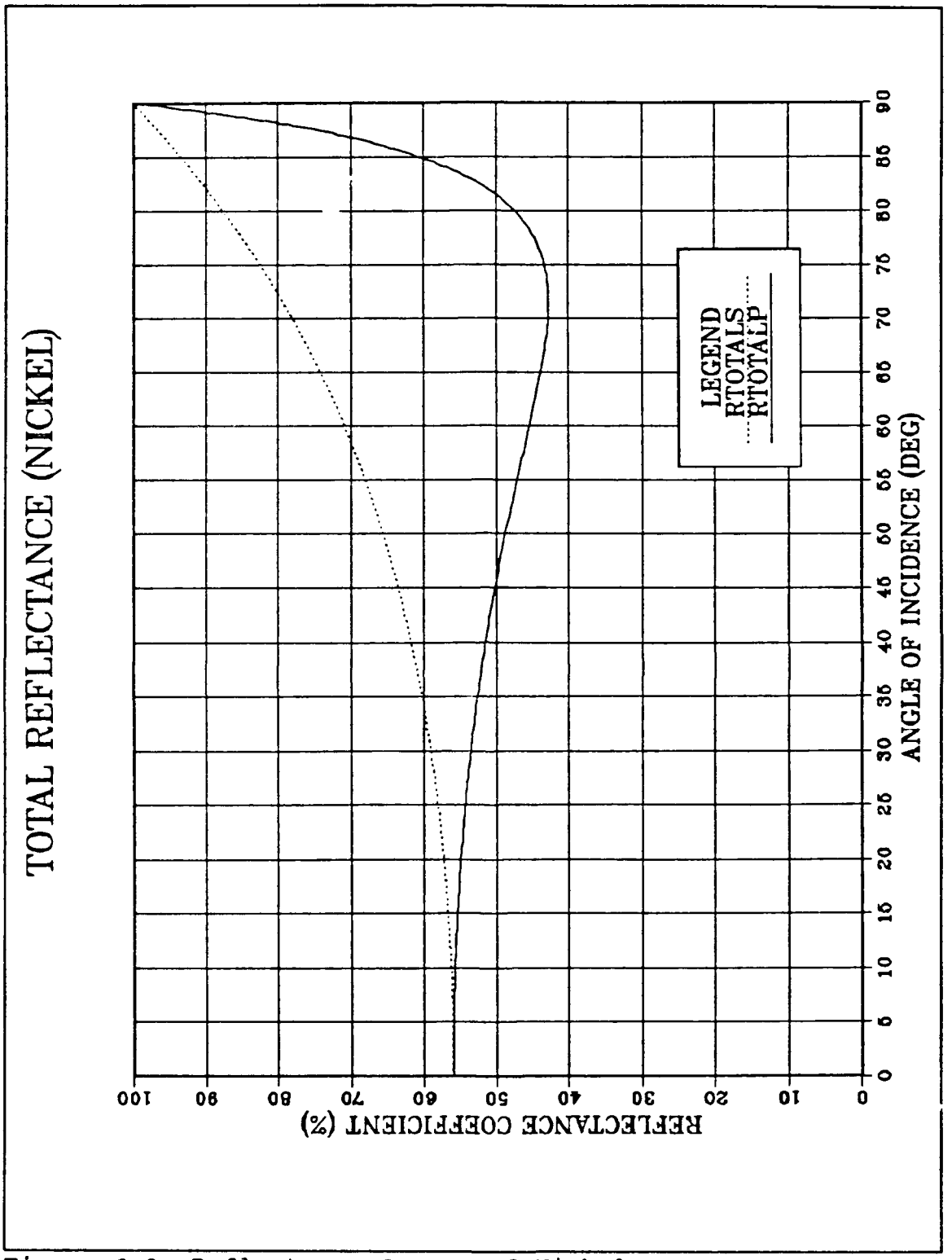


**Figure 6.3** Reflectance Curves Of Nickel.

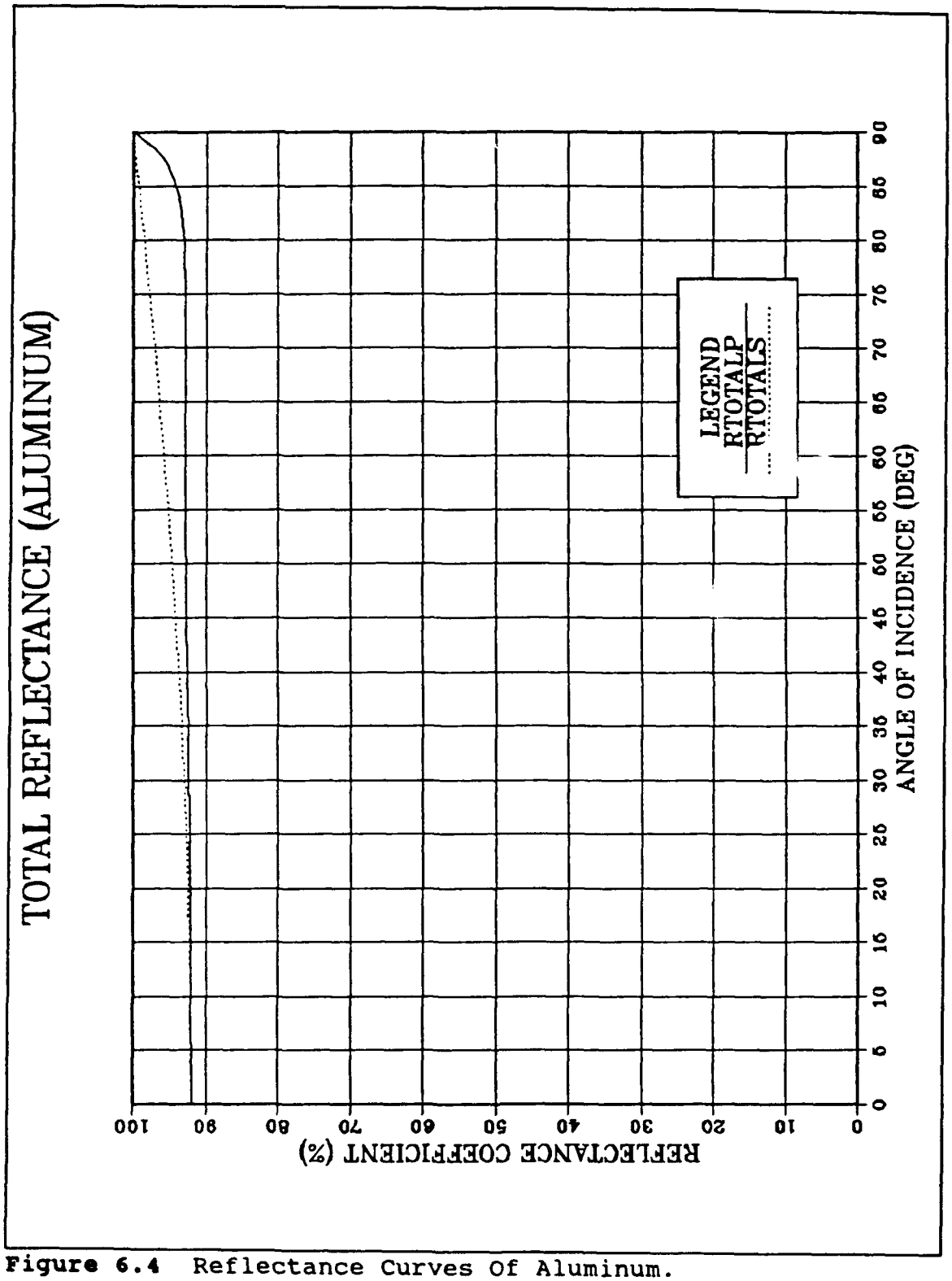


**Figure 6.4** Reflectance Curves Of Aluminum.

- At the grazing angle of incidence, both parallel and perpendicular reflectance are equal to unity as are the respective experimental values.

The cluster model is intended to permit agreement between experimental and cluster model values of reflectance, for two angles of incidence, $\phi$ ranging from 0° to 90°, as well as the angle of incidence where the perpendicular reflectance is at a minimum. However, for intermediate angles of incidence the reflectance values are determined by the cosine function as applied to Equations 5.3 and 5.4, when the parameters of n′, x, and emissivity are fixed. As a result the results of the model differ from experimental results in the following ways.

- Experimental parallel reflectance values are greater than those predicted by the cluster model.
- Conversely, experimental perpendicular reflectance values are less than corresponding values determined by the cluster model.

## B. TABULATION OF THE KEY PARAMETERS

The values for index of refraction (n′), cluster to bulk surface area ratio (x), and emissivity ($\epsilon$) are considered key elements in the development of the model since, it is these values which are metal property dependent and in large part account for the manner in which light is reflected from the metal. In this work non-spectral equations were used. Table 6.1 below, lists the values of each parameter arrived at by the iteration process given in the computer algorithm development in Chapter V.

Table 6.1 KEY CLUSTER-MODEL PARAMETERS OF METALS

| Metal Name | Emissivity ($\epsilon$) | Index of refraction (n') | Surface Area Ratio (x) |
|---|---|---|---|
| Gold | 0.04674 | 2.6696 | 0.6074 |
| Nickel | 0.08800 | 3.0710 | 0.5663 |
| Silver | 0.03998 | 3.1265 | 0.0865 |
| Aluminum | 0.05216 | 5.6479 | 0.0607 |

## C. ANALYSIS OF THE PARAMETERS

The index of refraction for gold and silver, as computed by the model (Table 6.1) is consistent with experimentally obtained values. Therefore this portion of the model development appears to be validated. From Table 6.1 one may note that the value of the surface area ratio (x) decreases as a function of an increasing normal reflectance. One can postulate that as the total reflectance at normal incidence increases this could be accounted for by a diminishing contribution from the cluster, due to less cluster surface area thereby allowing more of the surface area to act as a metallic grey body.

## D. SIZE OF CLUSTERS VERSUS PLOTS OF "n" AND "k"

Determining the size of the clusters is an important step in delineating which portion of the energy spectrum would be most susceptible to the cluster polarization model. Electromagnetic waves whose wavelengths are smaller than the size of the cluster (i.e., X-rays)would not see the surface clusters but the interior bulk metal. Conversely, electromagnetic waves which are much larger in wavelength than the cluster (i.e., long IR and larger) will not be effected by the cluster as the would tend to be

reflected as from an electric conductor. As postulated in Ref. 3, the size of the cluster is expected to be around one micrometer. Evidence of this may be supported by observing the experimental spectral plots of n and k for various metals over the energy spectrum. Tables 6.2 thru 6.5 are excerpts from tables given in Ref. 10 which will help validate the postulate.

**Table 6.2 COPPER [Ref. 10]**

| Wavelength ($\mu$m) | n | k |
|---|---|---|
| 0.5166 | 1.12 | 2.60 |
| 0.5390 | 1.04 | 2.59 |
| 0.5635 | 0.826 | 2.60 |
| 0.5904 | 0.468 | 2.81 |
| 0.6880 | 0.213 | 4.05 |
| 1.240 | 0.433 | 8.46 |

**Table 6.3 GOLD [Ref. 10]**

| Wavelength ($\mu$m) | n | k |
|---|---|---|
| 0.4592 | 1.426 | 1.846 |
| 0.5166 | 0.608 | 2.120 |
| 0.6888 | 0.160 | 3.80 |
| 0.7749 | 0.174 | 4.86 |
| 1.033 | 0.272 | 7.07 |
| 1.240 | 0.372 | 8.77 |

Table 6.4 SILVER [Ref. 10]

| Wavelength ($\mu$m) | n | k |
|---|---|---|
| 0.3155 | 1.044 | 0.514 |
| 0.3237 | 0.616 | 0.609 |
| 0.3306 | 0.371 | 0.813 |
| 0.4769 | 0.132 | 2.72 |
| 1.033 | 0.226 | 6.99 |
| 1.879 | 0.600 | 11.4 |

Table 6.5 TUNGSTEN [Ref. 10]

| Wavelength ($\mu$m) | n | k |
|---|---|---|
| 0.03815 | 0.797 | 0.286 |
| 0.05209 | 0.483 | 0.598 |
| 0.06812 | 0.766 | 1.19 |
| 1.265 | 3.15 | 4.36 |
| 2.138 | 1.18 | 8.44 |
| 6.199 | 3.87 | 28.3 |

From the above tables one will note that the value of n changes rapidly for all the metals around the 0.3 $\mu$m to 1.0 $\mu$m range, except for tungsten which displays two ranges of wavelength where n changes rapidly. Further, from the graphs of these plots [Ref. 10] given in Appendix D, one will note that while tungsten has two ranges of anomalies the only anomaly for the other metals is in the range of wavelength stated above. This would seem to indicate that some other mechanism of reflection is in effect over the range of wavelengths near one micrometer, and that mechanism could be a result of

interaction of the electromagnetic wave with the cluster surface. It is stated in Ref. 1 that in the portion of the energy spectrum which is in the near infrared it is difficult to measure the optical properties because of the "anomalous skin effect" [Ref. 9]. However, since all the metals, except tungsten, display a similar variance of n in the same wavelength range, it is difficult to dismiss the possibility that the cluster size is about 1$\mu$m.

# VII SUMMARY AND CONCLUSIONS

## A. MODEL COMPARISON

Explaining polarization upon reflection from metallic surfaces is not completely understood [Ref. 1]. As examples of this, one need only note that there exists various models each pertaining to a specific portion of the energy spectrum, which have been developed in an attempt to explain the results of reflection rather than mechanisms. For instance, the Drude model (i.e., free-electron theory), shows agreement with experimental results in the long infrared and longer wavelength portion of the spectrum where the interaction with the bound electrons can be ignored. However, this model begins to break down in the near infrared and shorter wavelength portions of the energy spectrum. In fact Ref. 5 states just this and refers the reader to the quantum model. The quantum model better describes polarization in the ultraviolet region of the spectrum. As stated in Ref. 1 this model only partially explains the polarization mechanism for this region.

The native cluster model, as formulated, fills the gap between the other two models, and expansion to encompass other regions of the spectrum seems to be restricted by the cluster's physical properties (i.e., size and the fact that they reside on the surface). Although still undergoing development, the formulation offers a mechanism for polarization in the near visible and visible portions of the spectrum. From the above, one can postulate that the answer to the fundamental problem of polarization upon

metallic reflection will require all three models because of the complex nature in which different energy waves interact with free and bound electrons of the conductor.

## B. MODEL EFFECTIVENESS

Values of non-spectral reflectance, as determined by the native cluster model, are within 10 % of the measured values throughout the range of angles of incidence. The variance between the model and experimental results, while not a constant, is consistent in direction. That is, the perpendicular value of reflectance from Ref. 7 is somewhat less than the value calculated by the model (see Figures 6.1 and 6.2), and conversely the parallel reflectance from Ref. 7 is somewhat greater than that of the model. This consistency in the direction of the variance gives rise to the possibility that the model, as it currently stands, is incomplete. It will be remembered that, from Chapter II, the indirect reflection from within the cluster was not accounted for in the calculations.

However, the model does generate curves with the same characteristics and shape. More precisely the generated curves have the same values at normal and grazing angles of incidence and the same angle of incidence defined earlier to be the pseudo-Brewster angle. This gives the model validity and a measure of effectiveness for predicting the reflectance curves of "white" light from various metallic surfaces.

The calculation of n′ based on the pseudo-Brewster angle appears to be correct in that it and the index of refraction as given by the free electron model are in close agreement. This could become an important issue since virtually all listed references have pointed out that surface preparation of the metal is non-standardized but yet, crucial

in the measurement of the optical properties. This fact, coupled with the statement from Ref. 10 which says that the measurement of the optical constants is difficult in the range above the infrared portion of the energy spectrum due to the "anomalous skin effect", could make the present model a useful tool in helping to set a new standard for the preparation of metallic surfaces.

The current formulation is for non-spectral visible waves, but could be extended in order to accommodate a spectral source of light. This would be desirable from a validation standpoint, since the author found limited sources of data for non-spectral reflectance form metals, while finding an abundance of spectral data for both reflectance curves and optical properties.

## C. RECOMMENDATIONS

As stated in Section A of this chapter, with further validation and refinement, the native cluster model could be useful in filling the gap between the free electron model and the quantum model. It is important to note however, that the development of this model does not attempt to make other models of polarization obsolete, but rather offers an alternative mechanism for polarization.

More research needs to be performed on bound native clusters. New work could encompass development of new observation techniques. The ability to detect clusters and further observe their behavior over time with varying surface energies is needed. This would lead to answers concerning size, geometry, state, and perhaps migration or time evolution of the clusters.

## D. APPLICATIONS

According to Ref. 2, it may be possible to create made to order clusters with the most desirable electronic, magnetic and optical properties. If the native cluster model is factual, then it may be possible to alter the electron structure of the clusters by externally managing the energy balance of the surface thereby minimizing or maximizing polarization depending on the application. This would be useful when working with high energy lasers, where a minimum loss of intensity and or polarization management upon reflection from the metallic surface is desired.

Other possible applications would be in thermal control design of spacecraft where, by controlling the polarization of metallic surface reflections, one could maximize or minimize the absorptance and hence the emittance from the component surface. Using similar methods, management of high energy laser beams or enhancement of the properties of off-axis beam splitters would be possible. New understanding of well known phenomena open new vistas in applications.

## REFERENCES


1. Bennett, J. and Bennett, G., Chapter 10, *Handbook of Optics*, (Driscoll, W. Ed.) McGraw-Hill Book Company, 1978.

2. Duncan, M.A., and Rouvray,D.H., Microclusters, *Scientific American*, pp. 110-115, December 1989.

3. Biblarz, O., Modification to Thermal Emissions by Clusters on Their Own Metallic Surface, *Journal of Vacuum Science*, A8(1), pp. 127-133, January/February 1990.

4. Hayashi, C., Ultrafine Particles, *Physics Today*,p. 44-51, December 1987.

5. Borne, M., and Wolf, E., Chapter 13, *Principles of Optics*, 6th ed., Pergamon Press, 1980.

6. Biblarz, O., *Untitled Paper*, Naval Postgraduate School, 1990.

7. Jenkins, F., and White, H., *Fundamentals of Optics*, 4th ed., McGraw-Hill Inc.,1976.

8. Skilling, H., *Fundamentals of Electric Waves*, Robert E. Krieger Publishing Company, 1948.

9. Wooten, E., *Optical Properties of Solids*, Academic Press Inc., 1972.

10. Lynch, D., and Hunter, W.,Palik, E., p. 275-358, *Handbook of Optical Constants of Solids*, Academic Press. Inc., 1985.

# APPENDIX A

Program "Reflecta"

```
C      PROGRAM NAME:  REFLECTA
C      AUTHOR NAME:   C. W. BALDWIN
C      DEVELOPED:     6 APRIL 1991
C      LAST REVISION: 02 DECEMBER 91
C
  10   PROGRAM REFLECTA
C
C    PROGRAM REFLECTA IS DESIGNED AS A TOOL FOR THE STUDY
C    OF THE "NATIVE CLUSTER" MODEL AS IT PERTAINS TO METALS.
C    THE BASIS OF THIS PROGRAM IS THAT CLUSTERS ACT AS AN AGENT IN THE
C    PARTIAL POLARIZATION OF VISIBLE ELECTROMAGNETIC WAVES AND HENCE
C    SURFACE AREA OF THE METAL CAN BE DIVIDED INTO TWO PARTS, THAT
C    COMPOSED OF THE CLUSTER AND THE REMAINDER OF BULK MATERIAL.
C    BY COMBINING THE REFLECTANCE FROM BOTH SURFACE AREAS THE
C    TOTAL REFLECTANCE IS CALCULATED FOR PARALLEL AND PERPENDICULAR
C    COMPONENTS.  THE THEORY BEHIND THIS MODEL IS GIVEN IN A THESIS
C    BY C. W. BALDWIN DATED DEC. 1991
C
C    REFLECT1 IS THE DATA FILE FROM WHICH THE PLOTS OF REFLECTANCE
C    ARE GENERATED BY INVOCATION OF EASY-PLOT. NOTE ONE MUST RENAME
C    THE REFLECT1  FILE TO REFLECT1 DATA IN ORDER TO READ THE DATA INTO
C    EASY-PLOT
C
C     DECLARE ALL VARIABLES
C
  20   REAL PHI(100), PHIPRIME(100), RSDP(100), RSDS(100)
  25   REAL RB(100), RTOTLP(100), RTOTLS(100)
  30   REAL N, NPRIME, EPSLON, X
  31   REAL RTOTLP1(3),X1(3)
C
C     OPEN THE FILE REFLCT1
C
  35   OPEN (UNIT = 8, FILE = 'REFLECT1', STATUS = 'NEW')
C
C     SET ALL PARAMETERS
C
  40   N = 1.000
C    N IS THE INDEX OF REFRACTION OF THE INCIDENT MEDIUM (AIR)
C
  50   PHIMIN1 = 72.0
C     PHIMIN1 IS THE ANGLE OF INCIDENCE WHICH GIVES THE SMALLEST
C     EXPERIMENTAL PERPENDICULAR COMPONENT OF REFLECTANCE
C
  52   XS= 0.6667
C
C      XS IS THE INITIAL GUESS OF CLUSTER TO SURFACE RATIO
C
  53   RHO = 0.000002200
C
C      RHO IS THE RESISTIVITY OF THE METAL
C
  54   STEMP = 3000.00
C
C      STEMP IS THE SOURCE TEMPERATURE (LIGHT BULB, SUN ETC)
C
       RSTOT0 = 0.56
C
C     RSTOT0 IS THE EXPERIMENTAL REFLECTANCE AT 0DEG OF INCIDENCE
C

C  CALCULATION OF EMISSIVITY
C
C  RHO = RESISTIVITY (OHM-CM) FUNTION OF TEMP, KELVIN
C  STEMP = TEMP OF ILLUMINATING SOURCE KELVIN
C  GOOD FOR GREY OR BLACK BODIES
C
       EPSLON = 0.5753*((RHO*STEMP)**0.5)
C
C  CALCULATION OF NPRIME
C
C     NPRIME IS THE THEORETICAL VALUE OF INDEX OF REFRACTION OF THE
C     CLUSTER.
```

```
      PHIMIN = (3.14/180.0)* PHIMIN1
      NPRIME = TAN(PHIMIN)
C
C  CALCULATION OF X (CLUSTER TO SURFACE RATIO)
C
      PHIPRIM1 = ASIN((N/NPRIME) * 0.0349)
      RSDP1 = ((0.0349 - PHIPRIM1)/(0.0349+PHIPRIM1))**2
      RB1 = ( 1.0 - EPSLON * 0.9994)
      DO 75 J = 1,2
        DELTA = 0.05*J
        X1(J) = XS + DELTA
        RTOTLP1(J) = (1.0 - X1(J))*RB1 + (X1(J)*RSDP1)
  75  CONTINUE
C
C  CALCULATE SLOPE OF LINE
C
      R = (RTOTLP1(2) - RTOTLP1(1))/(X1(2) - X1(1))
      B = RTOTLP1(2) - R * X1(2)
      X = (RSTOTO - B)/R
      PRINT*, 'METAL TYPE IS NICKEL'
      PRINT*, 'EPSILON = ',EPSLON
      PRINT*, 'RHO = ',RHO
      PRINT*, 'STEMP = ',STEMP
      PRINT*, 'CLUSTER TO BULK RATIO = ',X
      PRINT*, 'NPRIME = ',NPRIME
      PRINT*
C
C     PRINT HEADER FOR OUTPUT
C
  55  PRINT 60
  60  FORMAT(4X,'PHI',5X,'PHI PRIME',4X,'RSDP',6X,'RSDS',3X,'RB',
     *8X,'RTOTLP',3X,'RTOTLS')
C
C
C     INITIATE LOOP TO VARY PHI(I) FROM 0 - 90  DEGREES
C
  70  DO 104 I = 1,92,2
  72     PHI(I) = ((-1.0+I)*(3.14/180.0))
         IF (PHI(I) .EQ. 0.0) THEN
           PHIPRIME(I)=RSDP(I)=RSDS(I)=RB(I)=0.00
           GOTO 104
           ELSE
           CONTINUE
          ENDIF
  80     PHIPRIME(I) = ASIN ((N/NPRIME)*(SIN(PHI(I))))
  90     RSDP(I) = ((TAN(PHI(I)-PHIPRIME(I)))/(TAN(PHI(I)+PHIPRIME(I))
     +   ))**2*100.0
 100     RSDS(I) = ((SIN(PHI(I)-PHIPRIME(I)))/(SIN(PHI(I)+PHIPRIME(I))
     +   ))**2*100.0
 101     RB(I) =( 1.0 - EPSLON*COS(PHI(I)))*100.0
 102     RTOTLP(I) = (1-X)*RB(I) + X*RSDP(I)
 103     RTOTLS(I) = (1-X)*RB(I) + X*RSDS(I)
C
 104     CONTINUE
         DO 140 I = 1,92,2
C        WRITE DATA TO DATA FILE REFLECT1
C
C        CONVERT PHI(I) AND PHIPRIME(I) FROM RADIANS TO DEGREES
C
 105     PHI(I) = PHI(I)*(180.0/3.14)
C
 106     PHIPRIME(I) = PHIPRIME(I)*(180.0/3.14)
         RTOTLP(1) = RTOTLP(3)
         RTOTLS(1) = RTOTLS(3)
 110     WRITE (8,120) PHI(I),PHIPRIME(I),RSDP(I),RSDS(I),RB(I)
     +   ,RTOTLP(I),RTOTLS(I)
 120     FORMAT(1X,F8.3,1X,F8.3,1X,F8.3,1X,F8.3,1X,F8.3,1X,F8.3
     +   ,1X,F8.3)
 140  CONTINUE
 145  CLOSE (UNIT = 8,STATUS = 'KEEP')
C
C        PRINT OUT DATA
```

```
C
 146  OPEN (UNIT = 8,FILE = 'REFLECT1',STATUS = 'OLD')
 150  DO 175 I = 1, 46
         READ (8,155) PHI(I), PHIPRIME(I), RSDP(I), RSDS(I),RB(I),
     *   RTOTLP(I), RTOTLS(I)
 155     FORMAT(1X,F8.3,1X,F8.3,1X,F8.3,1X,F8.3,1X,F8.3,1X,F8.3
     *   ,1X, F8.3)
 160     WRITE(6,170) PHI(I), PHIPRIME(I), RSDP(I), RSDS(I), RB(I),
     *   RTOTLP(I), RTOTLS(I)
 170     FORMAT(1X,F8.3,2X,F8.3,2X,F8.3,2X,F8.3,2X,F8.3,2X,F8.3,2X,F8.3)
 175  CONTINUE
 180  END
```

# APPENDIX B

Reflectance Data For Gold, Silver, Aluminum, Nickel

METAL TYPE IS GOLD
EPSILON = 0.0467576
RHO = 2.2000004E-06
STEMP = 3000.0000000
CLUSTER TO BULK RATIO = 0.6073907
NPRIME = 2.6696081

| PHI | PHI PRIME | RSDP | RSDS | RB | RTOTLP | RTOTLS |
|---|---|---|---|---|---|---|
| 0.000 | 0.000 | 0.000 | 0.000 | 0.000 | 49.989 | 50.012 |
| 2.000 | 0.749 | 20.682 | 20.720 | 95.329 | 49.989 | 50.012 |
| 4.000 | 1.497 | 20.625 | 20.777 | 95.338 | 49.958 | 50.050 |
| 6.000 | 2.244 | 20.531 | 20.871 | 95.352 | 49.906 | 50.113 |
| 8.000 | 2.988 | 20.398 | 21.005 | 95.372 | 49.833 | 50.202 |
| 10.000 | 3.730 | 20.227 | 21.178 | 95.397 | 49.739 | 50.317 |
| 12.000 | 4.467 | 20.017 | 21.390 | 95.428 | 49.624 | 50.458 |
| 14.000 | 5.199 | 19.768 | 21.644 | 95.465 | 49.487 | 50.627 |
| 16.000 | 5.926 | 19.479 | 21.940 | 95.507 | 49.328 | 50.823 |
| 18.000 | 6.647 | 19.150 | 22.280 | 95.555 | 49.147 | 51.048 |
| 20.000 | 7.361 | 18.780 | 22.665 | 95.608 | 48.944 | 51.303 |
| 22.000 | 8.067 | 18.369 | 23.097 | 95.666 | 48.717 | 51.589 |
| 24.000 | 8.764 | 17.916 | 23.579 | 95.730 | 48.466 | 51.906 |
| 26.000 | 9.452 | 17.419 | 24.112 | 95.799 | 48.192 | 52.257 |
| 28.000 | 10.129 | 16.880 | 24.700 | 95.873 | 47.893 | 52.643 |
| 30.000 | 10.795 | 16.296 | 25.344 | 95.952 | 47.570 | 53.065 |
| 32.000 | 11.450 | 15.668 | 26.049 | 96.036 | 47.221 | 53.526 |
| 34.000 | 12.092 | 14.994 | 26.817 | 96.124 | 46.847 | 54.028 |
| 36.000 | 12.720 | 14.276 | 27.653 | 96.218 | 46.447 | 54.572 |
| 38.000 | 13.334 | 13.512 | 28.560 | 96.316 | 46.021 | 55.162 |
| 40.000 | 13.934 | 12.703 | 29.543 | 96.419 | 45.571 | 55.799 |
| 42.000 | 14.517 | 11.851 | 30.606 | 96.526 | 45.095 | 56.487 |
| 44.000 | 15.084 | 10.956 | 31.755 | 96.637 | 44.595 | 57.228 |
| 46.000 | 15.633 | 10.022 | 32.996 | 96.752 | 44.073 | 58.027 |
| 48.000 | 16.165 | 9.052 | 34.333 | 96.871 | 43.530 | 58.886 |
| 50.000 | 16.678 | 8.050 | 35.774 | 96.994 | 42.970 | 59.810 |
| 52.000 | 17.171 | 7.024 | 37.325 | 97.121 | 42.397 | 60.802 |
| 54.000 | 17.643 | 5.983 | 38.994 | 97.251 | 41.816 | 61.866 |
| 56.000 | 18.095 | 4.940 | 40.788 | 97.385 | 41.235 | 63.008 |
| 58.000 | 18.525 | 3.912 | 42.715 | 97.521 | 40.664 | 64.232 |
| 60.000 | 18.933 | 2.922 | 44.783 | 97.661 | 40.117 | 65.544 |
| 62.000 | 19.318 | 1.995 | 47.003 | 97.804 | 39.613 | 66.948 |
| 64.000 | 19.679 | 1.184 | 49.383 | 97.949 | 39.175 | 68.450 |
| 66.000 | 20.016 | 0.530 | 51.933 | 98.097 | 38.836 | 70.057 |
| 68.000 | 20.328 | 0.108 | 54.664 | 98.247 | 38.638 | 71.775 |
| 70.000 | 20.615 | 0.013 | 57.586 | 98.399 | 38.640 | 73.609 |
| 72.000 | 20.876 | 0.375 | 60.710 | 98.553 | 38.921 | 75.568 |
| 74.000 | 21.111 | 1.369 | 64.049 | 98.709 | 39.585 | 77.656 |
| 76.000 | 21.320 | 3.235 | 67.612 | 98.866 | 40.781 | 79.883 |
| 78.000 | 21.501 | 6.311 | 71.414 | 99.025 | 42.711 | 82.254 |
| 80.000 | 21.656 | 11.067 | 75.464 | 99.185 | 45.663 | 84.777 |
| 82.000 | 21.782 | 18.181 | 79.776 | 99.346 | 50.047 | 87.459 |
| 84.000 | 21.881 | 28.637 | 84.361 | 99.508 | 56.461 | 90.308 |
| 86.000 | 21.952 | 43.901 | 89.231 | 99.670 | 65.796 | 93.330 |
| 88.000 | 21.995 | 66.211 | 94.398 | 99.833 | 79.411 | 96.532 |
| 90.000 | 22.010 | 99.086 | 99.871 | 99.996 | 99.443 | 99.920 |

METAL TYPE IS SILVER
EPSILON = 0.0399823
RHO = 1.6100003E-06
STEMP = 3000.0000000
CLUSTER TO BULK RATIO = 0.0864533
NPRIME = 3.1264963

| PHI | PHI PRIME | RSDP | RSDS | RB | RTOTLP | RTOTLS |
|---|---|---|---|---|---|---|
| 0.000 | 0.000 | 0.000 | 0.000 | 0.000 | 89.998 | 90.002 |
| 2.000 | 0.640 | 26.536 | 26.577 | 96.004 | 89.998 | 90.002 |
| 4.000 | 1.278 | 26.473 | 26.639 | 96.011 | 90.000 | 90.014 |
| 6.000 | 1.916 | 26.370 | 26.743 | 96.024 | 90.002 | 90.034 |
| 8.000 | 2.551 | 26.224 | 26.889 | 96.041 | 90.005 | 90.062 |
| 10.000 | 3.184 | 26.037 | 27.077 | 96.062 | 90.008 | 90.098 |
| 12.000 | 3.813 | 25.806 | 27.309 | 96.089 | 90.013 | 90.143 |
| 14.000 | 4.438 | 25.533 | 27.585 | 96.120 | 90.018 | 90.195 |
| 16.000 | 5.058 | 25.215 | 27.907 | 96.156 | 90.023 | 90.256 |
| 18.000 | 5.672 | 24.853 | 28.275 | 96.197 | 90.029 | 90.325 |
| 20.000 | 6.280 | 24.445 | 28.691 | 96.243 | 90.036 | 90.403 |
| 22.000 | 6.882 | 23.991 | 29.156 | 96.293 | 90.042 | 90.488 |
| 24.000 | 7.475 | 23.489 | 29.675 | 96.347 | 90.048 | 90.583 |
| 26.000 | 8.060 | 22.939 | 30.243 | 96.406 | 90.055 | 90.686 |
| 28.000 | 8.636 | 22.340 | 30.869 | 96.469 | 90.061 | 90.798 |
| 30.000 | 9.203 | 21.689 | 31.552 | 96.537 | 90.066 | 90.919 |
| 32.000 | 9.759 | 20.986 | 32.296 | 96.609 | 90.071 | 91.049 |
| 34.000 | 10.304 | 20.231 | 33.102 | 96.685 | 90.075 | 91.188 |
| 36.000 | 10.837 | 19.421 | 33.975 | 96.765 | 90.078 | 91.336 |
| 38.000 | 11.358 | 18.556 | 34.918 | 96.849 | 90.080 | 91.494 |
| 40.000 | 11.865 | 17.636 | 35.933 | 96.936 | 90.080 | 91.662 |
| 42.000 | 12.359 | 16.660 | 37.025 | 97.028 | 90.080 | 91.840 |
| 44.000 | 12.839 | 15.627 | 38.198 | 97.123 | 90.077 | 92.029 |
| 46.000 | 13.303 | 14.539 | 39.455 | 97.221 | 90.073 | 92.227 |
| 48.000 | 13.752 | 13.398 | 40.802 | 97.323 | 90.068 | 92.437 |
| 50.000 | 14.185 | 12.205 | 42.242 | 97.429 | 90.061 | 92.658 |
| 52.000 | 14.600 | 10.966 | 43.782 | 97.537 | 90.053 | 92.890 |
| 54.000 | 14.999 | 9.686 | 45.426 | 97.648 | 90.044 | 93.134 |
| 56.000 | 15.379 | 8.375 | 47.179 | 97.763 | 90.035 | 93.389 |
| 58.000 | 15.741 | 7.046 | 49.048 | 97.880 | 90.027 | 93.658 |
| 60.000 | 16.084 | 5.715 | 51.038 | 97.999 | 90.021 | 93.939 |
| 62.000 | 16.407 | 4.410 | 53.155 | 98.121 | 90.019 | 94.234 |
| 64.000 | 16.711 | 3.162 | 55.406 | 98.245 | 90.025 | 94.542 |
| 66.000 | 16.993 | 2.021 | 57.797 | 98.372 | 90.042 | 94.864 |
| 68.000 | 17.255 | 1.049 | 60.336 | 98.500 | 90.075 | 95.201 |
| 70.000 | 17.496 | 0.336 | 63.028 | 98.630 | 90.132 | 95.552 |
| 72.000 | 17.715 | 0.006 | 65.880 | 98.762 | 90.224 | 95.919 |
| 74.000 | 17.912 | 0.234 | 68.900 | 98.895 | 90.366 | 96.302 |
| 76.000 | 18.086 | 1.265 | 72.095 | 99.030 | 90.578 | 96.701 |
| 78.000 | 18.238 | 3.453 | 75.471 | 99.166 | 90.891 | 97.117 |
| 80.000 | 18.367 | 7.311 | 79.034 | 99.303 | 91.350 | 97.551 |
| 82.000 | 18.473 | 13.603 | 82.793 | 99.441 | 92.020 | 98.001 |
| 84.000 | 18.556 | 23.485 | 86.752 | 99.579 | 93.001 | 98.470 |
| 86.000 | 18.615 | 38.757 | 90.918 | 99.718 | 94.448 | 98.957 |
| 88.000 | 18.651 | 62.307 | 95.297 | 99.857 | 96.611 | 99.463 |
| 90.000 | 18.663 | 98.953 | 99.892 | 99.997 | 99.907 | 99.988 |

METAL TYPE IS ALUMINUM
EPSILON = 0.0521591
RHO = 2.7400001E-06
STEMP = 3000.0000000
CLUSTER TO BULK RATIO = 0.0607143
NPRIME = 5.6478672

| PHI | PHI PRIME | RSDP | RSDS | RB | RTOTLP | RTOTLS |
|---|---|---|---|---|---|---|
| 0.000 | 0.000 | 0.000 | 0.000 | 0.000 | 91.999 | 92.001 |
| 2.000 | 0.354 | 48.860 | 48.902 | 94.787 | 91.999 | 92.001 |
| 4.000 | 0.708 | 48.797 | 48.966 | 94.797 | 92.004 | 92.014 |
| 6.000 | 1.060 | 48.691 | 49.071 | 94.813 | 92.012 | 92.035 |
| 8.000 | 1.412 | 48.542 | 49.219 | 94.835 | 92.024 | 92.065 |
| 10.000 | 1.762 | 48.350 | 49.410 | 94.863 | 92.039 | 92.104 |
| 12.000 | 2.110 | 48.114 | 49.643 | 94.898 | 92.057 | 92.150 |
| 14.000 | 2.455 | 47.832 | 49.920 | 94.939 | 92.079 | 92.206 |
| 16.000 | 2.797 | 47.505 | 50.240 | 94.986 | 92.103 | 92.269 |
| 18.000 | 3.136 | 47.129 | 50.605 | 95.039 | 92.130 | 92.341 |
| 20.000 | 3.472 | 46.705 | 51.014 | 95.098 | 92.160 | 92.422 |
| 22.000 | 3.803 | 46.230 | 51.469 | 95.164 | 92.193 | 92.511 |
| 24.000 | 4.130 | 45.702 | 51.969 | 95.235 | 92.227 | 92.608 |
| 26.000 | 4.452 | 45.120 | 52.516 | 95.311 | 92.264 | 92.713 |
| 28.000 | 4.768 | 44.480 | 53.110 | 95.394 | 92.303 | 92.827 |
| 30.000 | 5.079 | 43.779 | 53.752 | 95.482 | 92.343 | 92.949 |
| 32.000 | 5.384 | 43.016 | 54.443 | 95.576 | 92.385 | 93.078 |
| 34.000 | 5.682 | 42.187 | 55.183 | 95.675 | 92.427 | 93.217 |
| 36.000 | 5.974 | 41.287 | 55.975 | 95.779 | 92.471 | 93.363 |
| 38.000 | 6.259 | 40.314 | 56.818 | 95.889 | 92.515 | 93.517 |
| 40.000 | 6.536 | 39.262 | 57.714 | 96.003 | 92.558 | 93.678 |
| 42.000 | 6.805 | 38.127 | 58.663 | 96.123 | 92.601 | 93.848 |
| 44.000 | 7.066 | 36.904 | 59.667 | 96.247 | 92.644 | 94.026 |
| 46.000 | 7.318 | 35.587 | 60.726 | 96.375 | 92.684 | 94.211 |
| 48.000 | 7.562 | 34.170 | 61.843 | 96.508 | 92.723 | 94.404 |
| 50.000 | 7.796 | 32.648 | 63.017 | 96.646 | 92.760 | 94.604 |
| 52.000 | 8.021 | 31.013 | 64.250 | 96.787 | 92.793 | 94.811 |
| 54.000 | 8.237 | 29.259 | 65.543 | 96.932 | 92.823 | 95.026 |
| 56.000 | 8.442 | 27.380 | 66.897 | 97.081 | 92.849 | 95.249 |
| 58.000 | 8.637 | 25.370 | 68.315 | 97.234 | 92.871 | 95.478 |
| 60.000 | 8.822 | 23.224 | 69.792 | 97.390 | 92.887 | 95.714 |
| 62.000 | 8.996 | 20.939 | 71.335 | 97.549 | 92.897 | 95.957 |
| 64.000 | 9.159 | 18.517 | 72.943 | 97.711 | 92.903 | 96.207 |
| 66.000 | 9.311 | 15.965 | 74.616 | 97.876 | 92.903 | 96.464 |
| 68.000 | 9.451 | 13.299 | 76.356 | 98.043 | 92.898 | 96.726 |
| 70.000 | 9.580 | 10.553 | 78.162 | 98.213 | 92.891 | 96.996 |
| 72.000 | 9.697 | 7.786 | 80.036 | 98.385 | 92.884 | 97.271 |
| 74.000 | 9.802 | 5.100 | 81.978 | 98.559 | 92.885 | 97.552 |
| 76.000 | 9.896 | 2.671 | 83.987 | 98.735 | 92.902 | 97.839 |
| 78.000 | 9.977 | 0.798 | 86.065 | 98.912 | 92.955 | 98.132 |
| 80.000 | 10.046 | 0.000 | 88.211 | 99.091 | 93.074 | 98.430 |
| 82.000 | 10.102 | 1.200 | 90.424 | 99.270 | 93.316 | 98.733 |
| 84.000 | 10.146 | 6.096 | 92.705 | 99.451 | 93.783 | 99.041 |
| 86.000 | 10.178 | 17.966 | 95.052 | 99.632 | 94.674 | 99.354 |
| 88.000 | 10.197 | 43.574 | 97.465 | 99.814 | 96.399 | 99.671 |
| 90.000 | 10.204 | 98.187 | 99.943 | 99.996 | 99.886 | 99.993 |

METAL TYPE IS NICKEL
EPSILON = 0.0467376
RHO = 2.2000004E-06
STEMP = 3000.0000000
CLUSTER TO BULK RATIO = 0.5662929
NPRIME = 3.0710201

| PHI | PHI PRIME | RSDP | RSDS | RB | RTOTLP | RTOTLS |
|---|---|---|---|---|---|---|
| 0.000 | 0.000 | 0.000 | 0.000 | 0.000 | 55.989 | 56.012 |
| 2.000 | 0.651 | 25.859 | 25.900 | 95.329 | 55.989 | 56.012 |
| 4.000 | 1.302 | 25.798 | 25.962 | 95.338 | 55.958 | 56.051 |
| 6.000 | 1.951 | 25.695 | 26.065 | 95.352 | 55.906 | 56.115 |
| 8.000 | 2.597 | 25.551 | 26.210 | 95.372 | 55.832 | 56.206 |
| 10.000 | 3.241 | 25.364 | 26.397 | 95.397 | 55.738 | 56.323 |
| 12.000 | 3.882 | 25.136 | 26.627 | 95.428 | 55.622 | 56.467 |
| 14.000 | 4.518 | 24.864 | 26.901 | 95.465 | 55.484 | 56.638 |
| 16.000 | 5.150 | 24.550 | 27.221 | 95.507 | 55.324 | 56.837 |
| 18.000 | 5.775 | 24.190 | 27.586 | 95.555 | 55.142 | 57.065 |
| 20.000 | 6.394 | 23.786 | 27.999 | 95.608 | 54.936 | 57.322 |
| 22.000 | 7.007 | 23.336 | 28.462 | 95.666 | 54.706 | 57.609 |
| 24.000 | 7.611 | 22.839 | 28.976 | 95.730 | 54.452 | 57.928 |
| 26.000 | 8.207 | 22.294 | 29.543 | 95.799 | 54.173 | 58.279 |
| 28.000 | 8.794 | 21.700 | 30.165 | 95.873 | 53.869 | 58.663 |
| 30.000 | 9.371 | 21.056 | 30.846 | 95.952 | 53.539 | 59.083 |
| 32.000 | 9.937 | 20.360 | 31.586 | 96.036 | 53.181 | 59.538 |
| 34.000 | 10.492 | 19.613 | 32.390 | 96.124 | 52.796 | 60.032 |
| 36.000 | 11.035 | 18.812 | 33.261 | 96.218 | 52.383 | 60.566 |
| 38.000 | 11.566 | 17.957 | 34.201 | 96.316 | 51.942 | 61.141 |
| 40.000 | 12.083 | 17.048 | 35.214 | 96.419 | 51.471 | 61.759 |
| 42.000 | 12.586 | 16.083 | 36.305 | 96.526 | 50.972 | 62.423 |
| 44.000 | 13.075 | 15.065 | 37.477 | 96.637 | 50.443 | 63.135 |
| 46.000 | 13.548 | 13.993 | 38.735 | 96.752 | 49.886 | 63.897 |
| 48.000 | 14.005 | 12.869 | 40.082 | 96.871 | 49.301 | 64.712 |
| 50.000 | 14.446 | 11.696 | 41.525 | 96.994 | 48.690 | 65.583 |
| 52.000 | 14.870 | 10.479 | 43.068 | 97.121 | 48.056 | 66.511 |
| 54.000 | 15.276 | 9.224 | 44.717 | 97.251 | 47.402 | 67.501 |
| 56.000 | 15.664 | 7.942 | 46.477 | 97.385 | 46.734 | 68.556 |
| 58.000 | 16.033 | 6.645 | 48.355 | 97.521 | 46.058 | 69.679 |
| 60.000 | 16.383 | 5.351 | 50.356 | 97.661 | 45.387 | 70.872 |
| 62.000 | 16.712 | 4.088 | 52.487 | 97.804 | 44.733 | 72.141 |
| 64.000 | 17.022 | 2.888 | 54.754 | 97.949 | 44.117 | 73.488 |
| 66.000 | 17.310 | 1.801 | 57.165 | 98.097 | 43.565 | 74.917 |
| 68.000 | 17.577 | 0.891 | 59.727 | 98.247 | 43.115 | 76.433 |
| 70.000 | 17.822 | 0.249 | 62.446 | 98.399 | 42.817 | 78.039 |
| 72.000 | 18.046 | 0.000 | 65.330 | 98.553 | 42.743 | 79.739 |
| 74.000 | 18.246 | 0.318 | 68.386 | 98.709 | 42.991 | 81.537 |
| 76.000 | 18.424 | 1.448 | 71.621 | 98.866 | 43.699 | 83.438 |
| 78.000 | 18.579 | 3.744 | 75.044 | 99.025 | 45.068 | 85.445 |
| 80.000 | 18.711 | 7.714 | 78.660 | 99.185 | 47.386 | 87.562 |
| 82.000 | 18.819 | 14.112 | 82.478 | 99.346 | 51.079 | 89.794 |
| 84.000 | 18.903 | 24.074 | 86.504 | 99.508 | 56.790 | 92.144 |
| 86.000 | 18.964 | 39.360 | 90.744 | 99.670 | 65.517 | 94.615 |
| 88.000 | 19.000 | 62.776 | 95.204 | 99.833 | 78.848 | 97.212 |
| 90.000 | 19.013 | 98.970 | 99.890 | 99.996 | 99.415 | 99.936 |

# APPENDIX C

## Spectral Plots of n and k

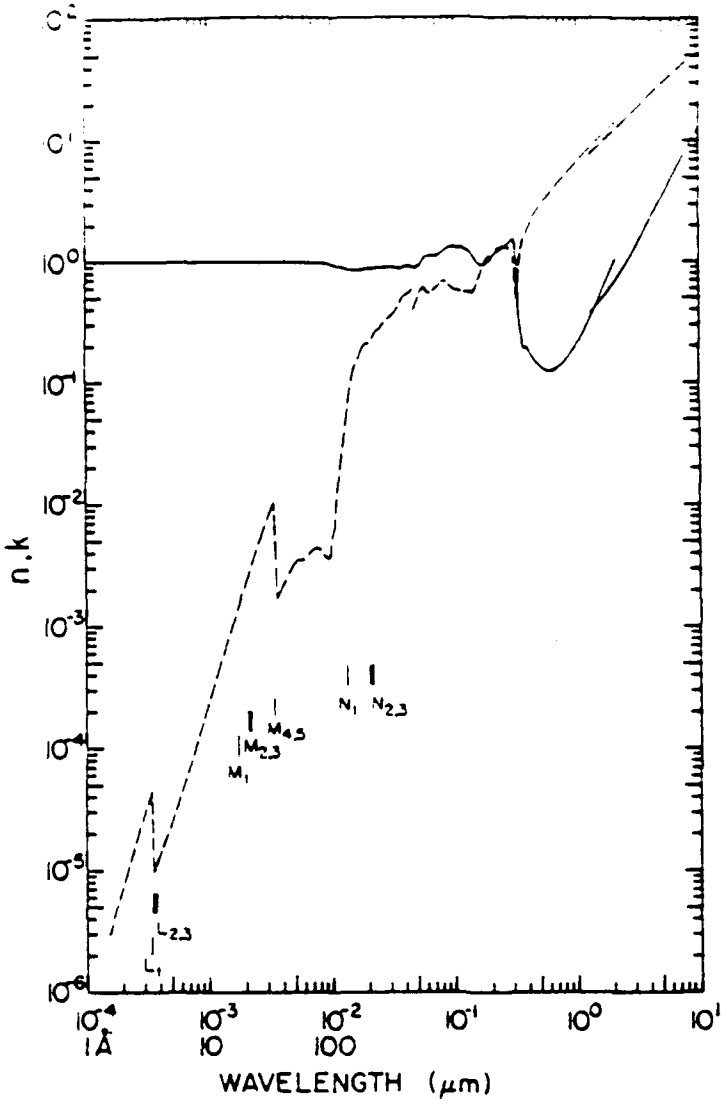


Plots of n (-) and k (- -) for
Copper [Ref. 10]

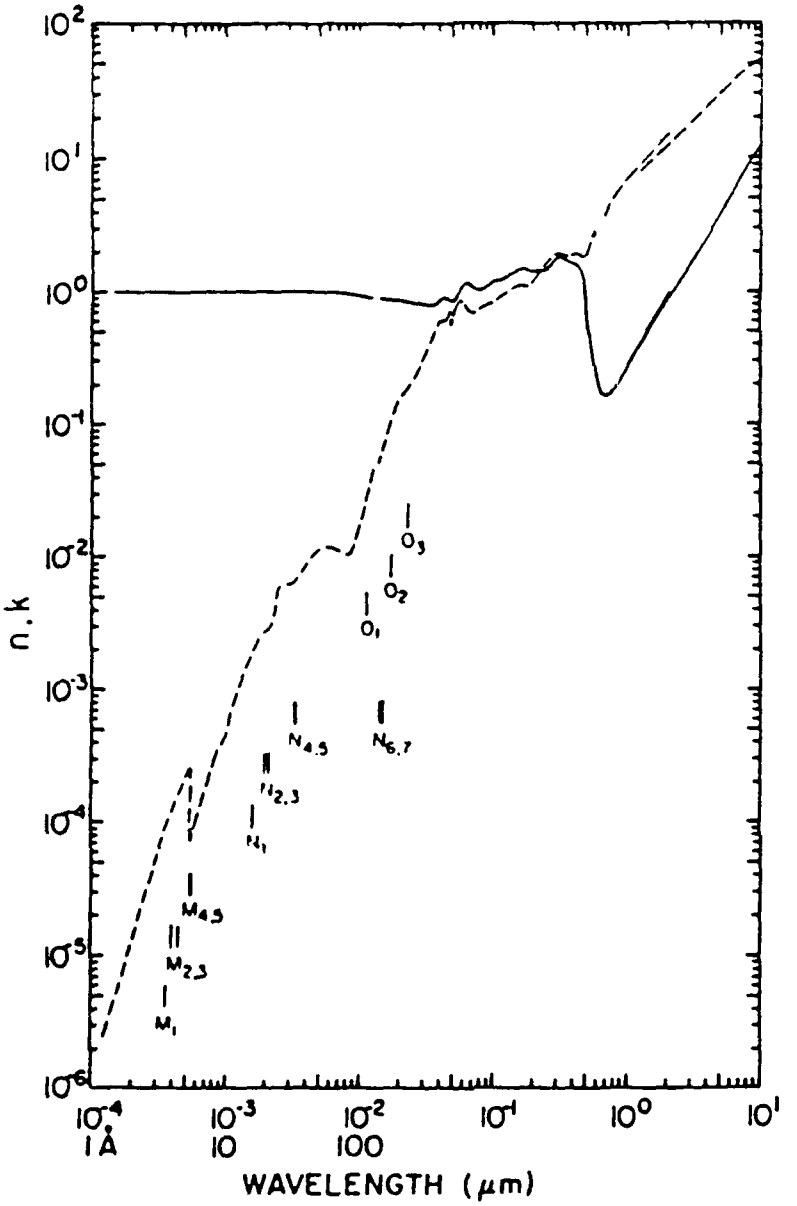


Plots of n (-) and k (- -) for
Gold [Ref. 10]

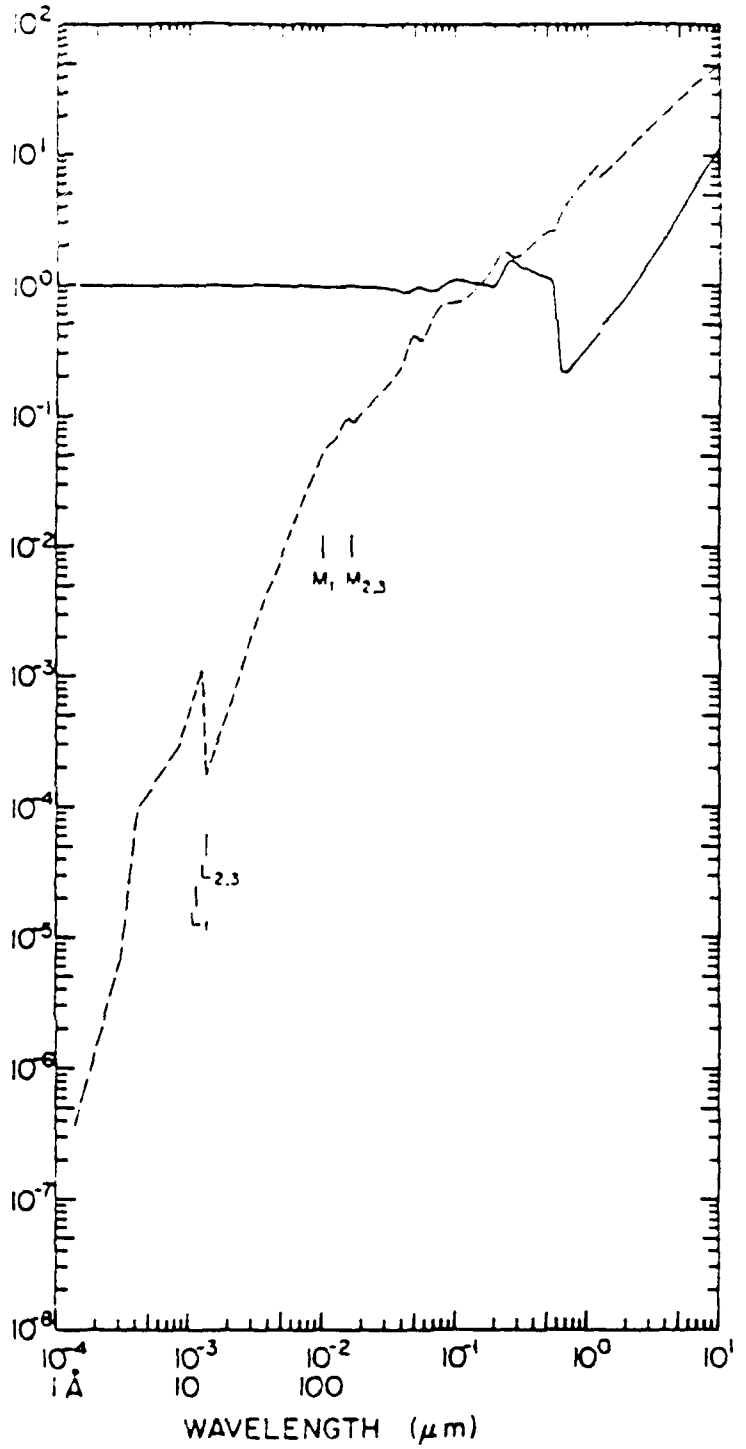


Plots of n (-) and k (- -) for
Silver [Ref. 10]

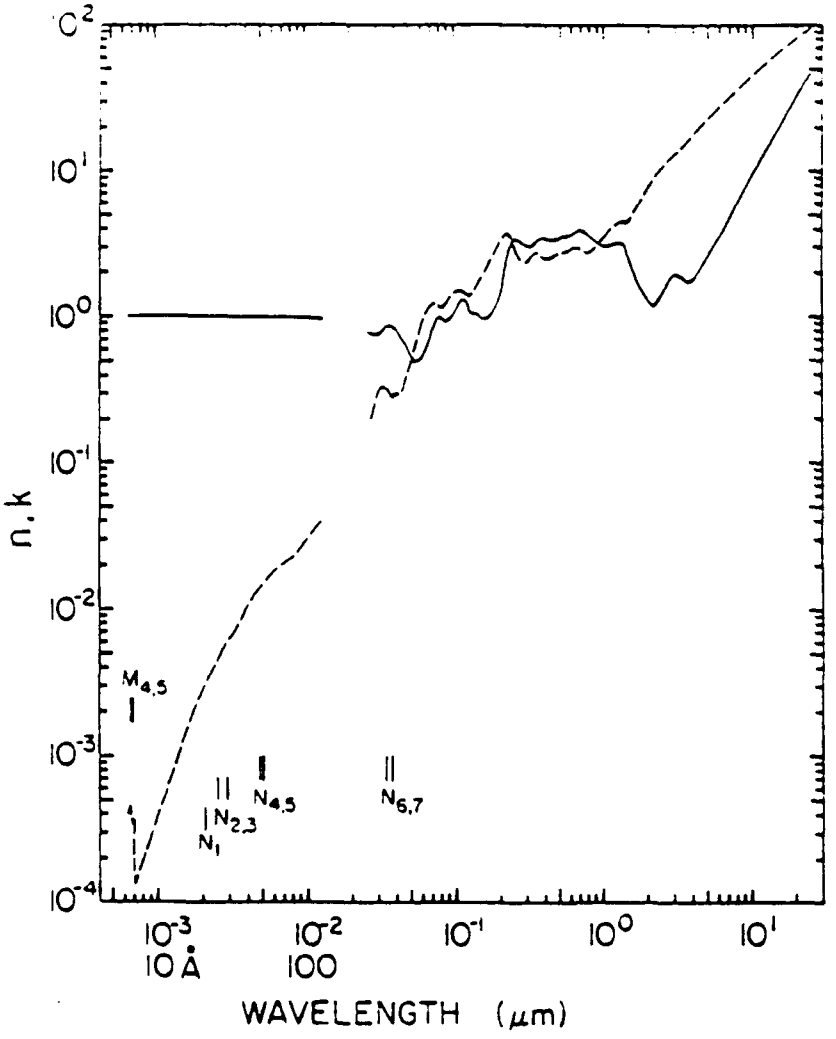


Plots of n (-) and k (- -) for
Tungsten [Ref. 10]

## INITIAL DISTRIBUTION LIST

| | No. Copies |
|---|---|
| 1. Defense Technical Information Center<br>Cameron Station<br>Alexandria, Virginia 22304-6145 | 2 |
| 2. Library, Code 52<br>Naval Postgraduate School<br>Monterey, California 93943-5002 | 2 |
| 3. Chairman<br>Department of Aeronautics and Astronautics, Code AA<br>Naval Postgraduate School<br>Monterey, California 93943-5000 | 1 |
| 4. Professor Oscar Biblarz<br>Department of Aeronautics and Astronautics, Code AA/Bi<br>Naval Postgraduate School<br>Monterey, California 93943-5000 | 4 |
| 5. Chairman<br>Space Systems Academic Group, Code SP<br>Naval Postgraduate School<br>Monterey, California 93943-5000 | 1 |
| 6. Professor Brij Agrawal<br>Department of Aeronautics and Astronautics, Code AA/Ag<br>Naval Postgraduate School<br>Monterey, California 93943-5000 | 1 |
| 7. Dr. J. Bennett Code 38103<br>Physics Division<br>Naval Weapons Center<br>China Lake, California 93555 | 1 |
| 8. Dr. D. Decker Code 3816<br>Physics Division<br>Naval Weapons Center<br>China Lake, California 93555 | 1 |

9. LCDR Craig Baldwin 2
2128 Subida Terrace
Rancho La Costa, California 92009